

1 **Running Head: Mechanosensitivity in plant roots**

2 **Corresponding Author: Rabi A. Musah**

3 **Address: Department of Chemistry**

4 **State University of New York at Albany**

5 **1400 Washington Avenue**

6 **Albany, NY 12222**

7 **Telephone: 518-437-3740**

8 **E-mail: rmusah@albany.edu**

9 **Research Area: Signaling and Response**

10

11

12

13

14

15

16

17

18

19

20

21 **Mechanosensitivity Below Ground: Touch-Sensitive Smell-**
22 **Producing Roots in the “Shy Plant,” *Mimosa pudica* L.**

23 Rabi A. Musah^{1*}, Ashton D. Lesiak¹, Max J. Maron¹, Robert B. Cody², David
24 Edwards², Kristen Fowble, A. John Dane², and Michael C. Long¹

25 ¹Department of Chemistry, University at Albany, State University of New York, 1400
26 Washington Avenue, Albany, NY 12222, USA.

27 ²JEOL USA Inc., 11 Dearborn Road, Peabody, MA 01960, USA.

28

29 *To whom correspondence may be addressed. E-mail: rmusah@albany.edu

30 **Summary:** Plant roots can exhibit a type of mechanosensitivity whereby they emit noxious
31 organosulfur compounds in response to touch.

32

33 **Author Contributions:** RAM conceived of the work, designed the experiments, conducted
34 experiments, interpreted the data and wrote the manuscript; ADL and RBC conducted mass
35 spectrometric measurements and RBC interpreted some of the resulting data; MJM conducted
36 GC-MS and various control experiments; DE conducted microscopy experiments; KF conducted
37 headspace analysis experiments; AJD conducted GC-MS experiments; ML germinated plant
38 seedlings.

39

40 **Financial source:** National Science Foundation grant number 1310350 to RAM and RBC.

41

42

43 **Financial source:** National Science Foundation grant number 1310350 to RAM and RBC.

44 **Corresponding Author:** Rabi A. Musah

45 rmusah@albany.edu

46

47

48

49

50

51

52

53

54

55

56

57

58

59

60

61

62

63

64 **ABSTRACT**

65 The roots of the “shy plant” *Mimosa pudica* L. emit a cocktail of small organic and inorganic
66 sulfur compounds into the environment, including SO₂, methylsulfinic acid, pyruvic acid, lactic
67 acid, ethanesulfinic acid, propane sulfinic acid, 2-aminothiophenol, S-propyl propane 1-
68 thiosulfinate, and thioformaldehyde, an elusive and highly unstable compound never before
69 reported to be emitted by a plant. When soil around the roots is dislodged or when seedling roots
70 are touched, an odor is detected. The perceived odor corresponds to emission of higher amounts
71 of propanesulfenic acid, 2-aminothiophenol, S-propyl propane 1-thiosulfinate, and
72 phenothiazine. The mechanosensitivity response is selective. Whereas touching the roots with
73 soil or human skin resulted in odor detection, agitating the roots with other materials such as
74 glass did not induce a similar response. Light and electron microscopy studies of the roots
75 revealed the presence of microscopic sac-like root protuberances. Elemental analysis of these
76 projections by energy dispersive X-ray spectroscopy revealed them to contain higher levels of K⁺
77 and Cl⁻ compared to the surrounding tissue. Exposing the protuberances to stimuli that caused
78 odor emission resulted in a reduction in the levels of K⁺ and Cl⁻ in the touched area. The
79 mechanistic implications of the variety of sulfur compounds observed vis-à-vis the pathways for
80 their formation are discussed.

81

82

83

84

85

86

87

88

89

90 INTRODUCTION

91 Plant roots are known to exude a diversity of both small and macromolecular chemicals
92 that mediate antimicrobial, anti-quorum sensing, allelopathic, and other effects (De-la-Peña et
93 al., 2012). However, the machinery associated with the synthesis and extrusion of these
94 compounds is not well understood. One of the most intriguing but least studied of these is
95 emission of volatile and reactive organosulfur compounds such as the foul and toxic gas carbonyl
96 sulfide (COS) and volatile carbon disulfide (CS₂). Both are reportedly released by numerous
97 plants and are proposed to make a significant contribution to the environmental sulfur burden
98 (Haines et al., 1989). As a case in point, the Central American rainforest plant *Stryphnodendron*
99 *exelsum* Harms (Mimosaceae), is a sufficiently strong sulfur emitter that its location in the forest
100 can be determined by odor (Haines et al., 1989). Furthermore, 40 taxa from nine genera within
101 the subfamily Mimosoideae, revealed that 29 from six genera produced CS₂, and 19 of the 40
102 taxa produced COS (Piluk et al., 2001). It has been proposed that the COS and CS₂ are derived
103 from a putative cysteine lyase-mediated cleavage of djenkolic acid, an amino acid previously
104 isolated from the plant (Piluk et al., 1998), but this has not been confirmed.

105 We used *Mimosa pudica* L. (Leguminosae), a perennial shrub endemic to Brazil but now
106 pantropical in its distribution (Howard, 1988), as a model to begin investigations of how this and
107 related plants emit these highly reactive and corrosive compounds without themselves incurring
108 tissue damage. Its various colloquial names, such as “sensitive plant,” “touch-me-not,” “shy
109 plant” and “humble plant,” among many others (Holm, 1977), derive from its seismonastic
110 movements—in response to touch, water, shaking, wind, or warming, its leaves quickly close,
111 slowly opening after an average of about 10 min (Song et al., 2014). It also displays nyctinasty,
112 with its leaves closing or “sleeping” with the onset of darkness. These curious characteristics
113 coupled with its small size have made the plant a convenient and popular attraction in schools,
114 greenhouses and other learning environments where it is used to illustrate seismonasty.

115 Our studies show that by using direct analysis in real time high-resolution mass
116 spectrometry (DART-HRMS) (Cody et al., 2005), it is possible to detect the compounds emitted
117 by plant roots *in situ*. Using this method, it was revealed that both *M. pudica* plants germinated
118 aseptically on agar and those germinated in soil emitted a variety of small molecules into the
119 atmosphere at levels that were not detectable by human subjects. However, an odor detectable by
120 humans could be sensed when the plant root was disturbed, with odor emission being dependent

121 on the nature of the stimulus. Analysis of the chemical contributors to the odor revealed that
122 although the array of compounds observed to be produced by the roots was the same both pre-
123 and post- stimulation, emission of a subset of organosulfur compounds was increased when the
124 roots were stimulated. Light and scanning electron microscope imaging studies revealed the
125 presence of sac-like protuberances dotted along *M. pudica* seedling root shafts that collapsed
126 when the roots were exposed to stimuli that elicited odor emission. The detection by energy
127 dispersive X-ray spectroscopy of relatively high levels of K^+ and Cl^- prior to root stimulation on
128 the one hand, and reductions in the levels of these species on the other, implicates the
129 involvement of these ions in the observed mechanostimulatory behavior.

130

131 **RESULTS**

132 ***M. pudica* seedlings emit organosulfur compounds into the environment**

133 In previous studies where odor emission from *M. pudica* roots was reported (Hartel and
134 Haines, 1992; Hartel and Reeder, 1993; Piluk et al., 1998), roots from gnotobiotically grown
135 plants were detached from the aerial parts, washed with water, and subsequently crushed in an
136 airtight plastic syringe. After a 7 min delay, the headspace of the crushed roots was analyzed by
137 GC-MS. The only compound detected by this method was CS_2 and therefore it was concluded
138 that the compound responsible for the odor detected when *M. pudica* is uprooted was CS_2 .

139 From these studies, it remained unclear whether the CS_2 observed was emitted by the
140 roots *in situ*, or appeared as a consequence of the root tissue breach. Therefore, we first
141 conducted headspace analysis of intact *M. pudica* seedlings to determine whether CS_2 was
142 present in the absence of tissue rupture, and to determine the optimal conditions for its detection
143 by DART-HRMS. For these experiments, *M. pudica* seeds were germinated aseptically on agar
144 so that they could be handled without tearing the roots. Seeds began germinating within 2-3
145 days, and seedlings grew to approximately 23 mm in length by the end of the first week. Over
146 that time frame, each plant produced a single tap root that did not have hairs visible to the naked
147 eye (Supplementary Figure S1). Using sterile stainless steel tweezers, seedlings were transferred
148 to sterile vials equipped with septum caps (1 seedling per vial, see Supplementary Figure S2). In
149 each case, the tweezers were used to grip the seedling at the hypocotyl. The transfer was
150 accomplished in ~10 sec. The seedling headspace was then immediately sampled for 5 min using
151 a PDMS solid phase microextraction (SPME) fiber (Supplementary Figure S2), and the fiber was

152 subsequently analyzed by DART-HRMS in both positive and negative-ion modes.
153 Representative results are shown in Figure 1. The positive-ion mode mass spectrum (Panel a)
154 included peaks at nominal m/z 93, 110, 167, and 184 whose exact masses corresponded to
155 formulas C_3H_9OS , C_6H_8NO , $C_6H_{15}OS_2$, and $C_6H_{18}NOS_2$ respectively. The formulas that
156 contained sulfur were consistent with those of a number of organosulfur compounds common to
157 *Allium* species such as onion, most notably propane sulfenic acid (m/z 93), and *S*-propyl propane
158 1-thiosulfinate in both protonated and ammoniated forms (m/z 167 and 184 respectively). The
159 thiosulfinate serves as the major odor and flavor molecule produced in freshly cut onions, and
160 the sulfenic acid is the reactive intermediate precursor of the thiosulfinate. The identity of the
161 thiosulfinate was confirmed by comparing the DART-HRMS mass spectral fragmentation
162 patterns of authentic standards obtained under in-source collision-induced dissociation (CID)
163 conditions (cone voltage of 90 V), to fragments observed by DART-HRMS analysis of the *M.*
164 *pudica* root samples under similar in source CID conditions. As sulfenic acids are fleeting
165 reactive intermediates that cannot be isolated, it was not possible to confirm the structural
166 identity of the peak at m/z 93. Thus, the propane sulfenic acid structural assignment is putative,
167 albeit informed by the observations outlined in published studies showing that this sulfenic acid
168 is the direct precursor of the *S*-propyl propane 1-thiosulfinate observed in this work and also seen
169 in onion (Block, 1992). Furthermore, Block et al. have observed this intermediate in onion using
170 DART-HRMS (Block et al., 2010; Block et al., 2011).

171 Figure 1 Panel b shows the DART-HRMS results of headspace analysis of the seedling in
172 negative-ion mode. Notable peaks included those at nominal m/z 60, 61, 91, 124, 165 and 198
173 whose exact masses corresponded to formulas N_2O_2 , HCO_3^- , C_3H_7SO , C_6H_6NS , $C_6H_{13}OS_2$ and
174 $C_{12}H_8NS$ respectively. Formula C_3H_7SO is consistent with the presence of the deprotonated
175 counterpart of the sulfenic acid intermediate putatively identified in the positive-ion mode
176 spectrum shown in Panel a. However, as stated previously, its identity cannot be confirmed
177 because it is a reactive intermediate as reported on extensively by Block et al. (Block, 1992).
178 While $C_6H_{13}OS_2$ corresponded to the deprotonated form of the thiosulfinate observed in the
179 positive-ion mode spectrum, the C_6H_6NS formula was consistent with that of an
180 aminothiophenol (*ortho*-, *meta*- or *para*), and the $C_{12}H_8NS$ corresponded to phenothiazine. In
181 order to confirm these tentative structural assignments, authentic standards of *ortho*-, *meta*- and
182 *para*-aminothiophenol, as well as an authentic standard of phenothiazine were subjected to in-

183 source CID by DART-HRMS in negative-ion mode. The fragmentation patterns were then
184 compared with the *M. pudica* seedling spectrum acquired under identical conditions. The
185 fragmentation patterns observed showed that C₆H₆NS and C₁₂H₈NS corresponded to *o*-
186 aminothiophenol (also known as 2-aminothiophenol) and phenothiazine respectively.

187

188 **It was the roots and not the aerial parts of *M. pudica* that emitted organosulfur odor**
189 **volatiles**

190 In order to determine whether *M. pudica* aerial parts were contributing to the
191 organosulfur volatiles profile, a method was devised to permit analysis of the roots and aerial
192 parts separately, in a manner that prevented disruption of plant tissue. Under sterile conditions, a
193 bed of agar was suspended within a glass cylinder (Supplementary Figure S3 Panel a). The
194 bottom of the cylinder was sealed with a septum and sterile water was introduced (via syringe),
195 such that an air pocket remained between the agar and the water surface (Supplementary Figure
196 S3 Panel c). Deposition of a 3-day old aseptically germinated *M. pudica* seedling on the top
197 surface of the agar within the vertically mounted cylinder resulted in downward growth of the
198 root through the agar plug towards the water (Supplementary Figure S3 Panel c). Within 48 h,
199 the root eventually emerged from the bottom of the agar so that it was freely suspended in the
200 open air space between the bottom of the agar disk and the water level, without touching the
201 water, while the aerial part grew above the agar bed. In this way, the agar served to separate the
202 compounds emitted by the aerial and root parts and allowed them to be analyzed independently.
203 The root headspace was sampled with a PDMS SPME fiber by withdrawing the water from the
204 bottom of the glass cylinder and inserting the SPME fiber as described earlier. The aerial
205 headspace was sampled by sealing the top of the glass receptacle and inserting the SPME fiber as
206 described. Representative negative-ion mode DART-HRMS spectra of the headspace of the
207 separated *M. pudica* aerial and root parts are shown in Figure 2, rendered in a head-to-tail plot
208 format. The root headspace (top spectrum) showed a profile of compounds that was quite
209 different from that detected in the aerial headspace (bottom spectrum). Notably, none of the
210 compounds detected in the root headspace were observed in the aerial headspace, and vice versa.
211 In addition, organosulfur compounds including the propane sulfenic acid, 2-aminothiophenol, *S*-
212 propyl propane 1-thiosulfinate and phenothiazine detected in the DART-HRMS negative-ion
213 mode spectrum of the seedling (Figure 1 Panel b) were observed. The results indicated that

214 organosulfur compounds were emitted by the roots and not the aerial parts. Furthermore, since
215 the analysis was conducted under sterile conditions and without breaching the plant tissue,
216 neither the molecules detected in the aerial headspace nor those observed in the root headspace
217 were contributions from intracellular components or microbes.

218 ***M. pudica* roots emit an odor when exposed to certain stimuli**

219 In the course of these studies and in alignment with previous reports (Hartel and Reeder,
220 1993; Piluk et al., 1998) we detected a pungent, unpleasant sulfurous odor when 7-day old
221 gnotobiotically grown plants were dislodged from soil. However, more often than not, it was also
222 observed that when left undisturbed, neither seedlings germinated in soil, nor plants germinated
223 aseptically on agar, exhibited an odor detectable to the human subjects performing the
224 experiments. Furthermore, several human subjects reported that odor detection appeared to occur
225 as a function of exposure of seedling roots to some stimuli but not to others. For example,
226 touching the roots with fingers often elicited a strong odor, while exposure of roots to glass (e.g.
227 vials, stirring rods) or stainless steel (e.g. tweezers), did not. Because of these observations, a
228 preliminary assessment of the presence or absence of an odor detectable to human subjects was
229 conducted by a panel of 5 untrained subjects who were asked to indicate whether or not they
230 detected a “sulfurous” odor when roots of 7-day old seedlings gnotobiotically germinated on
231 agar were touched. The sulfurous odor was defined as the smell the panelist experienced when an
232 *M. pudica* seedling was dislodged from soil. The study was blind, in that the panelists were not
233 apprised of whether the roots they were examining were touched or untouched. The study was
234 performed by exposing the roots of 7-day old seedlings to the following 5 stimuli: a finger; soil;
235 glass; stainless steel; and wood. Panelists were allowed to smell the root within 15 sec of root
236 exposure to the stimulus, and asked to indicate whether or not they experienced an odor different
237 from agar. The experiments were performed in two ways. For all cases except exposure of the
238 root to soil, the stimulus was used to tap the root once as illustrated in Supplementary Video
239 SV1, where the root is tapped with a finger. The seedlings used were all germinated on the bed
240 of agar. In the case of soil, the root was dragged across the soil surface as is illustrated in
241 Supplementary Video SV2 in order to simulate the effect of soil disruption that we and others
242 observed resulted in odor release. Exposure of the seedlings to the various stimuli was conducted
243 in replicates of 5 (i.e. each panelist was exposed to a total of 5 seedlings per stimulus experiment,
244 as well as to a control which was comprised of a seedling germinated on agar which had not been

245 touched with any stimulus). The results, shown in Supplementary Figure S4, revealed that
246 whereas root exposure to soil or fingers was observed to produce an odor detectable to the
247 panelists most of the time (100% and 85% of the time respectively), root stimulation with glass
248 did not have that effect within experimental error. Odor detection by the panelists in response to
249 the other stimuli occurred to varying extents as indicated by the standard deviations of the results
250 (wood: 35 ± 19 ; and metal: 35 ± 25).

251

252 **The DART-HRMS-derived headspace profile of compounds produced in response to a** 253 **smell producing stimulus was similar to that observed in the absence of an odor producing** 254 **stimulus**

255 In order to determine how the profile of compounds observed to be emitted by *M. pudica*
256 seedlings in the absence of an odor producing stimulus (Figure 1 a/b) compared to that emitted
257 by stimulated roots, the headspace volatiles of: (1) 7-day old sterile finger-stimulated seedlings;
258 and (2) 3-month old soil bound plants in which the soil had been agitated by squeezing the pot
259 three times, were sampled by PDMS SPME and analyzed by DART-HRMS as described above.
260 Examples of typically observed positive- and negative-ion mode mass spectra are illustrated in
261 Figure 3 and Figure 4 respectively. Positive-ion mode spectra of the seedling and the 3-month
262 old adult plant are rendered in a head-to-tail plot (Figure 3), in which the top panel shows the
263 seedling spectrum and the bottom the adult plant spectrum. The comparison shows that the
264 profile of compounds observed in both cases is similar. Moreover, the observed organosulfur
265 compounds were also detected in the positive-ion mode spectrum of the unstimulated seedling
266 root (Figure 1a). The comparison of the negative-ion mode spectra of the seedling and 3-month
267 old plant (both stimulated) (Figure 4) showed both similarities and differences. Most notably,
268 several of the peaks below m/z 89 in the seedling spectrum were absent in the spectrum of the
269 adult plant. These included the peaks at nominal m/z 46, 61, 62, 64 and 79.

270

271 **Mass spectrometric analysis of seedling roots revealed emission of higher amounts of select** 272 **organosulfur compounds when roots were stimulated**

273 Our earlier described mass spectral analyses revealed that a cocktail of small molecules
274 including organosulfur volatiles, were emitted by *undisturbed M. pudica* plants even though an
275 odor was usually not detectable by human subjects (Figure 1 and Figure 2). To determine the

276 compounds responsible for the odor detected when roots were exposed to appropriate stimuli, 7-
277 day old unstimulated seedlings grown on agar were transferred to glass vials. For each analysis, a
278 SPME fiber was exposed to the headspace gas produced by a single plant for 5 min, and the fiber
279 was then analyzed by DART-HRMS in negative-ion mode. Subsequently, each seedling was
280 exposed to human skin in the manner shown in Supplementary video S1, and the DART-HRMS
281 analysis was repeated. The experiment was conducted in triplicate. As previously observed, the
282 same profile of compounds found in undisturbed plants (Figure 1) was seen, except that while
283 the detected levels of some compounds remained constant within experimental error, the relative
284 levels in the case of others was double as indicated by an increase in the ion counts observed by
285 mass spectrometry. This result is illustrated in Figure 5 which shows the difference in ion counts
286 for compounds emitted from untouched and touched roots (depicted in blue and red
287 respectively). The total ion counts for the peaks at nominal m/z 91, 124, 165, and 198 were
288 approximately double those observed in the unstimulated roots, $\pm 5\%$. These peaks corresponded
289 to propanesulfenic acid (m/z 91), 2-aminothiophenol (m/z 124), *S*-propyl propane-1-thiosulfinate
290 (m/z 165), and phenothiazine (m/z 198). The identity of the compound represented by m/z value
291 239 is unknown.

292

293 **CS₂, which has been proposed to be responsible for the smell of *M. pudica* roots, was never**
294 **detected under the soft ambient ionization conditions of DART-HRMS, but only under GC**
295 **conditions**

296 Despite previous reports that the odor emitted by *M. pudica* roots is caused by CS₂
297 (Hartel and Reeder, 1993; Piluk et al., 1998), we never detected CS₂ by DART-HRMS even
298 though we analyzed >100 seedling roots of different ages, under various growth conditions (in
299 soil and on agar), and at different periods in the growing season (spring, summer, fall and
300 winter). Since CS₂ was detected previously by GC-MS, we conducted GC-MS analyses of SPME
301 fibers exposed to *M. pudica* root volatiles for 5 min under conditions similar to those previously
302 reported (Piluk et al., 1998). Supplementary Figure S5 shows the GC-MS results typically
303 observed. The GC chromatogram appears in Panel a, and shows that only two species, one of
304 which was molecular oxygen, were detected. The identity of the second peak which appeared at
305 1.36 min was confirmed to be CS₂ based on the match between its EI mass spectral

306 fragmentation (Panel b) pattern and authentic CS₂. Thus, in contrast to what was detected by
307 DART-HRMS but consistent with previous observations, CS₂ was detected by GC-MS.

308

309 **Microscopy revealed sac-like root protuberances that became flattened after the roots were**
310 **touched with odor inducing stimuli**

311 The observed emission of a variety of compounds from *M. pudica* roots prompted us to
312 examine whether the roots might have structures analogous to the glandular trichomes observed
313 on the aerial parts of plant species that secrete essential oils. Thus, we examined the roots by
314 light microscopy. At 6X magnification, hair-like protuberances that appeared in clusters along
315 the length of the tap root were observed (Supplementary Figure S6).

316 To examine the morphology of the hair-like structures of untouched vs. touched roots, 7-
317 day old untouched and touched seedlings that were aseptically germinated on agar were further
318 examined by cryo scanning electron microscopy (cSEM). Seedlings were flash frozen with
319 liquid nitrogen just prior to analysis. Figure 6 shows representative images of unstimulated and
320 stimulated seedling roots. On some areas of the unstimulated root, a significant number of turgid
321 protuberances were present (Figure 6, Panel a). Magnification of the section enclosed in a square
322 in Panel a is shown in Panel b. Other segments of the root were only sparsely populated with
323 protuberances as shown in Panel c. Panel d shows an example of what was typically observed for
324 roots that were stimulated to produce an odor. The root previously had protuberances as
325 observed by light microscopy (Supplementary Figure S6), but after the root was tapped once by a
326 human finger, the protuberances in the touched area had collapsed (Panel d).

327 Figure 7 shows a representative SEM micrograph of an untouched *M. pudica* root that
328 was acquired under cryo conditions using a microscope equipped with an energy dispersive X-
329 ray spectrometer (EDS) for elemental analysis determination. The cSEM micrograph is shown in
330 Panel a. Each of the elements detected in the X-ray map is represented by a different color
331 (indicated in Panel b). The hue of the micrograph of the root segment shown in Panel a, reflects
332 the composite of the overlaid color-coded contributions of the elements detected. The map sum
333 spectrum of the elements detected and their relative amounts are shown in Panel c. The EDS
334 analysis revealed that besides the expected C, N and O contributions expected to be present in
335 living tissue, other elements detected included K, Cl, N, Ca, S, P and Mg at 13.1, 2.6, 2.5, 1.7,
336 1.4, 0.5, and 0.4 weight % respectively (Figure 7 Panel c). The amounts of K⁺ and Cl⁻ were

337 significant enough in some of the hairs that an outline reflecting the presence and topology of the
338 hairs in the cSEM image shown in Panel a, can be seen in the K^+ and Cl^- maps (Panel b). The
339 microscopic protuberances, which were flattened under the high vacuum conditions of the
340 experiment, varied in length from between 100 and 200 μm , and had a sac-like appearance, with
341 several having relatively high localized levels of K^+ and Cl^- as revealed by EDS.

342 Figure 8 (top panel) shows the cSEM micrograph of a root segment on a bed of agar
343 whose left side was exposed to a human skin and whose right side was untouched. The sacs that
344 were previously on the left side of the root (as observed by light microscopy) had collapsed,
345 consistent with our previous observations (Figure 6d). However, sacs still appeared on the right
346 side (untouched) of the root segment. EDS analysis was performed on the three sections of the
347 root labeled “Spectrum 1”, “Spectrum 2” and “Spectrum 3” of the micrograph shown in Figure 8
348 (upper panel) in order to assess the similarity of the elemental profile of stimulated versus
349 unstimulated root sections. The EDS map sum spectra illustrating the elemental compositions for
350 the three sections are shown in the bottom panel of Figure 8. Comparison of the three spectra
351 from the three root areas sampled showed that although the level of K^+ was similar for the
352 Spectrum 1 and Spectrum 2 areas (i.e. 6.0 ± 0.1 and 5.2 ± 0.1 weight % respectively), that in the
353 Spectrum 3 area (which was farthest away from the area that was touched) was almost double, at
354 10.8 ± 0.1 weight %). Similar trends were observed for Cl^- , Ca^{2+} and S. For the Spectrum 1 and
355 Spectrum 2 sampled areas that were close to the part of the root that was stimulated by exposure
356 to human skin, the Cl^- levels were 0.8 ± 0.1 and 0.7 ± 0.1 weight % respectively, whereas a Cl^-
357 level of 2.3 ± 0.1 weight % was observed in the Spectrum 3 area. For Ca^{2+} , the relative amounts
358 observed for the Spectrum 1, Spectrum 2 and Spectrum 3 areas of the root segment were $1.1 \pm$
359 0.1 , 1.2 ± 0.1 and 2.3 ± 0.1 weight % respectively, showing that the amount of Ca^{2+} in the
360 Sample 3 area was double that observed in the Spectrum 1 and 2 areas. The amount of S in the
361 Spectrum 3 area was 1.4 ± 0.1 weight %, whereas that for the Spectrum 1 and 2 areas was $0.9 \pm$
362 0.1 and 1.0 ± 0.1 weight % respectively, showing that the amount of S in areas 1 and 2 was
363 similar, while that in area 3 was higher. Quantitation (i.e. determination of the actual amounts of
364 the elements in stimulated versus unstimulated roots) could not be made because quantitation by
365 EDS requires that the sample be (1) perfectly flat; (2) homogeneous; and (3) infinitely thick to
366 the X-ray beam. Since plant roots do not fit these criteria, the actual amounts of the elements
367 could not be determined. Attempts were also made to perform quantitation using X-ray

368 fluorescence. However, these efforts were unsuccessful because the sample handling required to
369 conduct the experiment always resulted in emission of volatiles. Thus, it was not possible to
370 acquire “before touch” and “after touch” results that could be compared for *different* samples.
371 However, in order to confirm the reproducibility of the results, the experiment was repeated
372 several times, and in all cases, the same aforementioned trends were observed. Thus, another
373 example is shown in Supplementary Figure S7. The segment of the root shown above the line in
374 the cSEM micrograph is the untouched portion, while that below the line was touched with a
375 finger. The sections labeled “1”, “2” and “3” in the micrograph are those areas that were
376 analyzed by EDS, and the EDS results are shown beneath the cSEM micrograph and labeled
377 “Spectrum 1”, “Spectrum 2” and “Spectrum 3” respectively. Similar to the results presented in
378 Figure 8, the section of the root furthest from the touched area exhibited the highest levels of K^+
379 and Cl^- (5.7 and 0.8 weight % respectively), while the relative levels of these ions for the
380 touched area were 2.6 and 0.5 weight % respectively).

381

382 **DISCUSSION**

383 In this article, we describe our observation of four heretofore unreported phenomena: (1)
384 the emission of compounds from roots in response to a touch stimulus; (2) the ability of the root
385 to distinguish between different types of stimuli, such as responding to exposure to soil or the
386 touch of a finger but not to other stimuli; (3) emission and detection of highly reactive and
387 elusive organosulfur intermediates, including thioformaldehyde, in addition to other unique
388 species; and (4) the presence of sac-like microscopic protuberances along *M. pudica* root shafts.

389 The finding that *M. pudica* roots secrete increased levels of metabolites in response to
390 touch is particularly remarkable in light of the fact that the aerial parts of the plant are also touch-
391 sensitive. The sac-like protrusions that were revealed by light microscopy and cSEM to appear in
392 clusters along the root shaft, are reminiscent of the well-known glandular trichomes that have
393 been observed on the aerial parts of many plants, and which manufacture and emit a diversity of
394 secondary metabolites (Tissier, 2012). Root hairs with glandular morphologies that secrete small
395 molecule organics have been observed in sorghum (Netzly and Butler, 1986) and apple (Head,
396 1964) seedlings. However, those that appear in *M. pudica* may be most analogous to the
397 “exploding” glandular trichomes seen on aerial parts of *Sicana odorifera* (Kellogg et al., 2002)
398 and *Salvia blepharophylla* (Bisio et al., 1999) (and proposed to have been present in the extinct

399 seed fern *Blanzysperis praedentata*) (Krings, 2002; Krings et al., 2003) that release exudate in
400 response to touch.

401 Plant root tip cells exhibit a form of responsiveness to touch whereby they can
402 circumvent barriers encountered in soil that obstruct their downward trajectory. For example, in
403 *Arabidopsis*, the gravitropism normally displayed by plant roots is supplanted with a
404 thigmotropic response when the downward direction of growth is impeded by a barrier (Okada
405 and Shimura, 1990; Massa and Gilroy, 2003). However, the ability of roots to distinguish
406 between types of stimuli was surprising and to our knowledge is not a previously reported
407 phenomenon. Nevertheless, this behavior seems analogous to a characteristic of the aerial parts
408 of plants that exhibit mechanostimulatory activity. It was noted by Darwin (Darwin, 1880;
409 Darwin, 1893), for example, that although the carnivorous response of *Drosera rotundifolia* is
410 induced by contact between insect prey and the plant's tentacles, these same tentacles do not
411 respond to rain or wind. Some flowers are also known to explosively release pollen in response
412 to touch. For instance, male flowers of the orchid species *Catesetum saccatum* forcefully release
413 their pollen sacs in response to touch by an insect of the antennae at the center of the flower.
414 How the plants distinguish between the different forms of stimuli (e.g. insect vs. inanimate
415 object) is not fully understood, and we do not yet know the mechanism by which *M. pudica*
416 emits small molecules in response to various stimuli. Interestingly, although a single tap by a
417 finger of an *M. pudica* root reliably resulted in odor emission, the same was not true of other
418 odor eliciting stimuli. For example, exposing a root to soil by gently tapping it once on the soil
419 surface did not produce an odor, whereas dragging the root across the surface (as shown in
420 Supplementary video SV2) reliably produced a strong odor. Although the latter observation
421 implied that odor emission was a consequence of rupturing of the sacs that appeared along the
422 root shaft, this conclusion did not explain why a single tap on the root by a human finger
423 produced an odor, but a similar action with glass did not. Additional more extensive studies are
424 being conducted to investigate the mechanism of this phenomenon.

425 The composite of small-molecule species detected by high-resolution positive- and
426 negative-ion mode DART-HRMS provided an unprecedented glimpse of the *in situ* root
427 emissions, and further expands on the recently demonstrated utility of ambient ionization MS
428 techniques in the detection of plant derived organosulfur volatiles (Domin, 2014). These include
429 the demonstrations (Block et al., 2010; Block et al., 2011) (Kubec et al., 2010) that various

430 organosulfur intermediates that are formed when the tissues of onion (*Allium cepa*), garlic
431 (*Allium sativum*), *Allium sicutum* and *Petiveria alliacea* are injured, can be detected in real time
432 by DART-HRMS. Of particular relevance is the finding that the changing profile of organosulfur
433 exudates that occurs in *Brassica* spp. roots in response to herbivore attack or a tissue breach can
434 be monitored in real time by proton transfer reaction-mass spectrometry (PTR-MS) (Crespo et
435 al., 2012; Danner et al., 2012; van Dam et al., 2012; Samudrala et al., 2015). If conventional
436 metabolome analysis sample preparation methods had been used in these cases (e.g. plant tissue
437 disruption followed by solvent extraction and GC-MS analysis of the extract), it would not have
438 been possible to distinguish between compounds emitted into the environment by the roots, and
439 those that were intracellular. Furthermore, the solvent extraction step used in many conventional
440 analysis methods selects for the subset of compounds that are most well-solubilized in the
441 solvent used, and thus not all compounds present are detected. These factors underscore the
442 utility of these ambient ionization MS techniques as tools for the investigation of *in situ* plant
443 emissions in a manner that does not interfere with the biological processes of the system.

444 In order to confirm that organosulfur volatiles contributions were from the roots and not
445 the plant's aerial parts, a small growth chamber was designed in which a plug of agar separated
446 the aerial parts from the roots. When placed on the bed of agar, the seedling tap root grew
447 through the agar and emerged on the opposite side. This construct permitted independent
448 analysis of both the roots and aerial parts without disturbing the plant or disrupting of the plant
449 tissue. Furthermore, as the experiment was conducted under sterile conditions, there were no
450 microbe-derived contributions to the headspace volatiles. Using this method, we were able to
451 confirm that the aerial parts did not contribute detectable organosulfur volatiles.

452 As compared to hydrocarbons, organo-oxygen and organo-nitrogen compounds,
453 organosulfur molecules are well-known to have low odor thresholds (ppb for organosulfur
454 compounds vs ppm for organo- oxygen and nitrogen compounds) (Leonardos et al., 1969).
455 Therefore, we were surprised by the observation that plant roots emitted organosulfur volatiles
456 that were detectable by DART-HRMS in the absence of a stimulus, even though they were not
457 detectable to humans by smell. Since mass spectrometric analysis showed that human olfactory
458 detection was associated with an apparent doubling of the emission of a subset of root volatiles,
459 we conclude that emissions from non-stimulated roots were at levels below the ppb olfactory
460 threshold for the panelists in our study. It should be noted that the use of SPME fibers to sample

461 headspace gases served to concentrate the volatiles, which means that the level of compounds
462 detected by SPME analysis were much lower than was implied by our ability to detect their
463 presence on the fiber. Our observations also raise the possibility that there may have been some
464 odor compounds that went undetected by the form of analysis used in this study. In our
465 experiments, PDMS SPME fibers were used to concentrate the headspace gases so that their
466 constituents would be at high enough levels to be detected. The fibers were exposed to the
467 headspace for 5 min (as opposed to 30 min which is used when one wishes to saturate the fibers)
468 in order to be able to differentiate between the relative levels of emitted compounds. Thus, one
469 way in which to determine whether additional odor compounds were present would have been to
470 extend the exposure time of the SPME fiber to the headspace, in order to capture the maximum
471 range and levels of compounds possible. We conducted this experiment by exposing PDMS
472 SPME fibers to the headspace of numerous *M. pudica* roots (stimulated and unstimulated) for 30
473 min. Subsequent DART-HRMS analysis revealed chemical profiles identical to those obtained
474 for stimulated and unstimulated roots that had been exposed to PDMS fibers for 5 min (data not
475 shown). This result supports the premise that we detected most if not all of the detected
476 compounds. However, it is also possible that there may have been odor compounds present that
477 were not adsorbed to the PDMS fiber. To date, we have not found a commercially available
478 SPME fiber that enabled us to detect the diversity of compounds adsorbed to PDMS. Thus, we
479 have concluded that at a minimum, there were 5 compounds represented by nominal m/z 91, 124,
480 165, 198 and 239, whose increased emission from *M. pudica* roots in response to appropriate
481 stimuli was correlated with odor detection by human subjects.

482 Although odiferous organosulfur compounds featured heavily in this mix of emitted
483 molecules, noticeably absent was the CS₂ reported by Piluk *et al.* (Piluk *et al.*, 1998). Published
484 studies on the analysis of CS₂ production in Mimosoideae spp. are similar in that they have all
485 involved: (1) detection of CS₂ *after* root tissue disruption; (2) a significant time delay between
486 tissue disruption and CS₂ analysis; and (3) detection of CS₂ under high injector temperature
487 conditions (100-250 °C) (Haines, 1991; Hartel and Reeder, 1993; Feng and Hartel, 1996; Piluk *et*
488 *al.*, 1998), a factor known to result in rapid and facile degradation of labile organosulfur
489 compounds (Block, 2011). The fact that optimal CS₂ production has been observed only after
490 tissue disruption and a significant delay between tissue rupture and analysis time could mean that
491 the chemistry resulting in the appearance of CS₂ was subsequent to earlier stage reactions that

492 rapidly produced compounds that served as a first line of chemical defense and which were later
493 degraded to CS₂. Additionally, the GC conditions used for analysis of organosulfur compounds
494 are notorious for promoting reactions in the GC injection port which result in the production of
495 compound artifacts (Block, 2011). In light of this and our own observations outlined herein, it is
496 possible that the CS₂ previously reported is not produced by the plant *per se*, but is rather formed
497 from precursors which under the GC conditions used, degraded to form CS₂. This hypothesis is
498 supported by our observation that in contrast to the diversity of compounds detected by DART-
499 HRMS analysis of SPME fibers exposed to *M. pudica* root volatiles, GC-MS analysis under
500 published conditions as well as GC analysis of PDMS SPME fibers that had been exposed to the
501 headspace were the only conditions under which CS₂ was observed (Supplementary Figure S5).
502 This implies that these compounds, when previously observed by GC-MS, were artifacts of the
503 experimental protocol used for their detection (Haines et al., 1989; Farkas et al., 1992; Hartel and
504 Reeder, 1993; Feng and Hartel, 1996; Piluk et al., 1998).

505 Several of the compounds emitted by *M. pudica* roots are consistent with those that
506 would be expected from cysteine lyase-mediated degradation of djenkolic acid, a compound
507 detected in *M. pudica* roots (Piluk et al., 1998). A putative mechanism for the formation of these
508 volatiles from djenkolic acid is shown in Figure 9, and it accounts for the observation of
509 thioformaldehyde, pyruvate and ammonia. Thioformaldehyde, a fleeting unstable species under
510 ambient conditions (Solouki et al., 1976), is a constituent of interstellar clouds (Agúndez et al.,
511 2008). It has been formed by thermolysis, photolysis or vacuum pyrolysis of appropriate
512 precursors, and observed by microwave spectroscopy (Penn et al., 1978) or trapped in low-
513 temperature matrices for structural studies (Jacox and Milligan, 1975; Solouki et al., 1976;
514 Torres et al., 1982; Watanabe et al., 1991; Suzuki et al., 2007). Its detection (albeit in trace
515 amounts), like that of the sulfenic and sulfinic acids observed here and in recent studies of
516 *Alliums* by Block and co-workers (Block et al., 2010), is quite remarkable, and speaks to the
517 utility of DART-HRMS in the characterization of reactive organosulfur intermediates.

518 The mechanism by which the roots are responsive to touch is unclear. However, the
519 observation that untouched root hairs contain relatively high levels of K⁺ and Cl⁻ (Figure 8 and
520 Supplementary Figure S7) and that touched root segments have lower relative levels of K⁺ and
521 Cl⁻ compared to untouched sections of the same root (Figure 8 and Supplementary Figure S7)
522 may indicate that the process is similar in some ways to that which has been proposed to cause

523 movement in the aerial parts of the plant. *M. pudica* leaf closing in response to touch is
524 controlled by specialized structures called pulvini that appear at the base of the petioles.
525 Movement occurs when cells within the pulvini lose water and turgor, which has been proposed
526 to be triggered in part by transport of K⁺ and Cl⁻ ions in pulvini cells (Simons, 1981; Fromm and
527 Eschrich, 1988; Visnovitz et al., 2007; Volkov et al., 2010; Volkov et al., 2010; Volkov et al.,
528 2014).

529 The seismonasty exhibited by the aerial parts of *M. pudica* has been suggested to be a
530 defensive strategy whose suddenness may serve to scare or shake off intruders (Pickard, 1973),
531 give the appearance of a less voluminous meal (Braam, 2005), or make more apparent to would
532 be predators the menacing thorns sported by the plant stems (Eisner, 1981). However, the
533 purpose of the mechanostimulatory behavior of the roots and the role of the compounds emitted
534 are not immediately apparent. Given the inherent complexities of rhizosphere ecosystem biology,
535 further systematic studies will be necessary to determine the functions of the root protuberances
536 and the small molecule emissions. These are areas of continuing study in our labs.

537
538
539
540
541
542
543
544
545
546
547
548
549
550
551
552
553

554 MATERIALS AND METHODS

555 **Plants.** *M. pudica* seeds were obtained from Seedvendor.com. They were immersed in 70%
556 aqueous ethanol for 1 min, rinsed with sterile water, submerged in 3.075% sodium hypochlorite
557 (50% solution of Clorox, Oakland, CA) containing 0.05% Tween-20 for 10 min and rinsed 9x
558 with 23 °C sterile water. Seeds were placed in 70 °C sterile water for 16 h at 23 °C. Using sterile
559 tweezers, five to six seeds were placed on 100 x 15 mm or 150 x 15 mm petri dishes containing
560 1x Murashige & Skoog medium with vitamins (PhytoTechnology Laboratories, Shawnee
561 Mission, KS), and 44 mM sucrose solidified with 2% tissue culture-grade purified agar
562 (PhytoTechnology Laboratories). Seeds germinated within two to three days and were grown
563 under fluorescent lights with 16 h of light per day at 23 °C. *M. pudica* seeds germinated in soil
564 were first scarified by suspending them in 70 °C deionized water for 16 h at 23 °C. Using
565 tweezers, 3-4 seeds were placed within each receptacle in a 36 cell greenhouse kit according to
566 the manufacturer's specifications (Burpee & Co., Warminster, PA). Germination occurred within
567 4 days. Seedlings were transplanted 14 days after germination into Miracle Gro™ flower and
568 vegetable garden soil in 6 in pots under greenhouse conditions. Plants were watered daily.

569
570 **Headspace solid-phase microextraction (SPME) sampling.** A 2 cm 50/30 µm
571 Divinylbenzene/Carboxen/ Polydimethylsiloxane (DVB/CAR/PDMS) 24 gauge Stableflex fiber
572 (Sigma-Aldrich, St. Louis, MO. USA), mounted within a manual SPME fiber holder assembly
573 (Sigma-Aldrich), was used for analysis of headspace gases. SPME fibers were conditioned by
574 heating at 250 °C in a helium gas stream for 2 h just prior to analysis, and were subjected to mass
575 spectrometric analysis to confirm the absence of adsorbed species prior to sampling of headspace
576 gases. For seedling analysis, 1-week old plants that were aseptically germinated on the surface of
577 agar were gently lifted at the stem just beneath the cotyledons and immediately placed in a
578 15 mL clear glass vial (O.D. × H × I.D. 21 mm × 70 mm × 12 mm, thread 18-400) (Sigma-
579 Aldrich) which was capped with a Mininert® screw thread valve (Sigma-Aldrich). For root
580 stimulation experiments, the seedling root was touched with a finger as shown in Supplementary
581 Video SV1 prior to placing it in the vial. The process of touching the root and depositing it into
582 the vial took approximately 10-15 s. The manual SPME fiber assembly equipped with a
583 conditioned SPME fiber was then inserted into the valve of the Mininert® cap, and the fiber was
584 exposed to the headspace gases for 5 min at 25 °C. Mass spectrometric analysis of the fiber was

585 then conducted either by DART-HRMS or GC-MS. The headspace gases of adult plants were
586 sampled similarly. The entire potted plant was placed into a jar (1.88 L, 12 cm internal diameter,
587 21 cm in height) which was sealed with an airtight cap that was outfitted with a rubber septum
588 through with the SPME fiber assembly was inserted. After exposure to headspace volatiles for 5
589 min, the SPME fiber was retracted, the fiber assembly was removed, and the fiber was then
590 immediately subjected to MS analysis. Adult plant root stimulation experiments were conducted
591 similarly, except that the plant to be analyzed was uprooted from soil, the bulk of the soil was
592 gently removed, and the entire plant was deposited within the 1.88 L jar as described above.

593

594 **Separation of the *M. pudica* aerial and root parts for independent headspace sampling.**

595 An apparatus comprised of a Pyrex® glass rod (25.4 mm O.D.) and a Pyrex® cylindrical tube
596 (26.4 i.d, 30 mm o.d) [both purchased from Sci-Tech Glassblowing, Inc. (Moorpark, CA USA)]
597 was created (Supplementary Figure S3). Both the glass rod and tube were cut into 90 mm
598 sections. An O-ring (7/8x1 in) was placed on the middle of the rod. The rod was inserted into the
599 cylindrical tube and the O-ring served to allow the rod to reach only half-way into the tube. The
600 opposite open end of the tube was covered with foil and the entire set-up was sterilized.
601 Subsequently, approximately 5.5 mL of plant media, comprised of Murashige & Skoog medium
602 with vitamins (PhytoTechnology Laboratories, Shawnee Mission, KS USA), sucrose, and plant
603 cell culture tested agar (Sigma-Aldrich, St. Louis, MO USA), was poured into the open end of
604 the cylindrical tube. After it had solidified, the glass rod was removed, leaving behind a 1 mm
605 thick disc of agar. One end of tube was sealed with sterile rubber sleeve septum (12.7 bottom
606 I.D., 23.7 mm O.D.; Sigma-Aldrich, St. Louis, MO USA). An aseptically germinated 3-day old
607 *M. pudica* seeding was placed on the agar surface using sterile tweezers. Sterile water (20 mL)
608 was injected through the bottom septum and the open end of the tube was lightly covered with
609 sterilized parafilm to prevent the agar from drying out. Within 48 h, seedling root had emerged
610 from the opposite side of the agar disk, such that the agar served to completely separate the
611 headspace of the aerial and root parts. To sample the root headspace, the water was withdrawn
612 via syringe and the PDMS SPME fiber was inserted into the septum. For sampling of the aerial
613 headspace, a rubber septum was applied to the top of the tube and the PDMS SPME fiber was
614 inserted into the septum. Sampling and analysis occurred as described above.

615

616 **Mass spectrometric analysis.** An AccuTOF™-DART (JEOL USA Inc., Peabody, MA USA)
617 high-resolution time-of-flight mass spectrometer (TOF-MS) was used for mass measurements.
618 The instrument and experimental conditions for the DART-TOF-MS analyses were conducted at
619 250 °C and performed as previously described (Kubec et al., 2010), except that headspace gases
620 were first adsorbed onto a SPME fiber, which was then analyzed. For analysis, the fiber was held
621 for a few seconds at the mass spectrometer inlet, and the resulting spectrum was recorded.
622 Calibration, spectral averaging, background subtraction, and peak centroiding of the mass spectra
623 were performed using TSSPro3 (Shrader Software Solutions, Detroit, MI, USA) data processing
624 software. Mass Mountaineer software (www.mass-spec-software.com, Toronto, Ontario,
625 Canada) was used for mass spectrum analysis, spectral elemental composition and isotope
626 analysis. Calibration was performed using a polyethylene glycol mixture (PEG 200, 400, 600,
627 and 1000). Experiments in which changes in the emission profiles of molecules were monitored
628 (to compare unstimulated and stimulated roots) were acquired in negative-ion mode. The
629 experiments were conducted in triplicate. Mass to charge ratio values for molecules whose
630 unstimulated versus stimulated ion counts were different within experimental error were selected
631 in TSSPro and subjected to peak area integration for each SPME fiber analysis. Reconstructed
632 ion chromatograms (RICs) of these peaks for each sample were exported to Excel. The total peak
633 area counts for the individual m/z values were calculated for each sample and then summed to
634 get the overall peak area counts. The three replicate individual peak area counts were averaged
635 and the average overall peak area count was calculated. GC-MS analysis was conducted using
636 an Agilent HP 6890 GC coupled to a HP 5972A mass selective detector (Agilent Technologies,
637 Santa Clara, CA, USA). Headspace gases from root-stimulated plants were sampled and
638 analyzed as previously described (Haines, 1991) using a capillary column (HP-5 MS, 30m x
639 0.25mm, 0.25 μ m), under the following conditions: Oven temp: 50 °C, raised linearly at a rate of
640 20 °C/min to 200 °C; Inlet temperature: 100 °C; Inlet mode: splitless; Carrier gas: He, with a
641 flow rate of 1 mL/min; Ionization mode: EI⁺, 70 eV, 300 μ A.

642
643 **Microscopy.** Scanning electron microscopy imaging of untouched and touched seedlings was
644 done under cryo conditions (cSEM) at liquid N₂ temperature. Two methods (1 and 2) were used:
645 *Method 1:* A 1-week old seedling was carefully placed onto an SEM sampling block (JEOL) that
646 was outfitted with two clamps that were used to hold the seedling in place. The entire setup was

647 then plunged into a Dewar of liquid N₂ where it was allowed to equilibrate. The sampling block
648 with the seedling was then viewed with a JSM-6610LV scanning electron microscope (JEOL
649 USA Inc.). With the samples prepared in this way, the turgor of the roots was maintained for a
650 significant period during the analysis (as illustrated in Figure 4).

651 *Method 2:* An SEM sampling block (JEOL USA Inc.) was immersed in liquid N₂ for 15 min.
652 The block was then removed from the liquid N₂ and a 1-week old seedling was contact-frozen by
653 quickly placing it onto the liquid N₂-cooled SEM sampling block. The sample was then imaged
654 using a JSM-IT300LV scanning electron microscope (JEOL USA Inc.).

655 *Light microscopy:* *M. pudica* roots were viewed using a Nikon stereozoom SMZ800 microscope
656 that was equipped with a Nikon DS Fi2 microscope camera.

657

658 **X-ray fluorescence.** X-ray fluorescence measurements were made with a JEOL JSX-1000
659 benchtop energy-dispersive X-ray fluorescence spectrometer.

660

661 **Root stimulation experiments.** The roots of *M. pudica* seedlings that were germinated
662 aseptically on agar were lifted from the agar bed with stainless steel tweezers at the stem beneath
663 the cotyledon and exposed to human skin and soil as shown in Supplemental Videos SV1 and
664 SV2 respectively. To determine whether exposure to other forms of matter elicited an odor
665 detectable to humans, roots were touched with the following materials either by a single tap with
666 the material as shown in SV1, or in the case of soil, by dragging the root across the surface as
667 shown in SV2: a 12 x 0.2 inch metal spatula (410 stainless steel, Fisher Scientific, Waltham
668 MA); a 6 x 0.19 in glass stirring rod (Fisher Scientific, Waltham MA); and a 4 in wooden
669 toothpick (Diamond L'Elegance extra long toothpicks, no additives) were used as stimuli. For
670 some experiments, exposure of roots to the metal, glass and wood stimuli was performed while
671 the roots were being viewed using a Nikon stereozoom SMZ800 microscope in order to
672 determine whether the structures along the root shaft were modified on exposure to the various
673 materials. For other experiments, roots were imaged by cSEM both before and after exposure to
674 human skin.

675

676 **Odor detection.** Odor emission from 7-day old *M. pudica* seedlings was assessed by a panel of 5
677 individuals who evaluated the samples as either having no detectable odor or a detectable odor.

678 Each panelist was exposed to 5 seedlings before and after stimulation. Seedlings were suspended
679 approximately 1 inch from the nose of each panelist before and after root stimulation.

680

681 **Odor emission experiments.** Odor emission from 7-day old *M. pudica* seedlings could be
682 elicited by dragging seedling roots across the surface of soil or subjecting the seedling to single
683 tap by a human finger (as shown in Supplementary video files SV2 and SV1 respectively). For
684 the soil experiments, 30 grams of Miracle Gro garden soil was dispensed into a petri dish bottom
685 (100 x 25 mm polystyrene dish, PhytoTechnology Laboratories, Shawnee Mission, KS). One
686 week old *M. pudica* seedlings were carefully lifted from agar plates at the seedling stem just
687 beneath the cotyledon with stainless steel tweezers. Seedling roots were then dragged along the
688 soil surface while being held with the tweezers (Supplementary video SV2). For the human
689 finger touch experiments, 7-day old *M. pudica* seedlings were tapped once with a finger as
690 shown in Supplementary video SV1. To test whether an odor could be detected if the seedling
691 root was exposed to other forms of matter, seedling roots were tapped once with: (a) a 6 x 0.19
692 in glass stirring rod (Fisher Scientific, Waltham MA); (b) a 12 x 0.2 in metal spatula (410
693 stainless steel, Fisher Scientific, Waltham MA); a 4 in wooden toothpick (Diamond L'Elegance
694 extra-long toothpicks, no additives). The influence of stimulation of the aerial plant parts on
695 detection of an odor was also determined. The cotyledons of 7-days old seedlings whose roots
696 had not been exposed to odor emission stimuli were held between the thumb and forefinger for
697 from 5 to 30 second and released. Whether or not an odor was detected was then recorded.

698

699

700

701

702

703

704

705

706

707 **FIGURE LEGENDS**

708 **Figure 1. Typically observed DART-HRMS positive- and negative-ion mode spectra of the**
709 **headspace of 7-day old *M. pudica* seedlings in the absence of an odor producing stimulus.** In
710 each case, a SPME fiber was exposed to the headspace for 5 min, and the fiber was then
711 analyzed by DART-HRMS. The structures shown are consistent with the observed HR elemental
712 compositions and isotope data obtained, as well as the results of comparisons of the
713 fragmentation patterns observed for standards under in-source CID conditions, to that of the
714 headspace samples also obtained under in-source CID conditions. Detected compounds were
715 observed in their protonated or ammoniated forms. The mass measurements and relative peak
716 abundances associated with the data shown here are presented in Table S1.

717
718 **Figure 2. Head-to-tail plot of the typically observed negative-ion mode DART-HRMS of the**
719 **headspace gases produced by the root (top spectrum) and aerial part (bottom spectrum) of**
720 **a 1-week old *M. pudica* plant.** The aerial and root parts were separated by an agar partition
721 within a Pyrex tube. In each case, a SPME fiber was exposed to the headspace gases for 5 min,
722 and the fiber was then analyzed by DART-HRMS. The structures shown are consistent with the
723 observed HR elemental compositions and isotope matching data, as well as the results of in-
724 source CID experiments. The mass measurements and relative peak abundances associated with
725 the data shown here are presented in Table S1.

726
727 **Figure 3. Head-to-tail plot of the typically observed positive-ion mode DART-HRMS of the**
728 **headspace gases produced by stimulated roots of: (1) 1-week old (Panel a); and (2) 3-month**
729 **old (Panel b) *M. pudica* plants.** In each case, a SPME fiber was exposed to the headspace gases
730 for 5 min, and the fiber was then analyzed by DART-HRMS. The structures shown are
731 consistent with the HR elemental compositions and isotope data obtained. Detected compounds
732 were observed in their protonated or ammoniated forms. The mass measurements and relative
733 peak abundances associated with the data shown here are presented in Table S3.

734
735 **Figure 4. Head-to-tail plot of the typically observed high-resolution (HR) negative-ion**
736 **mode DART-HRMS of the headspace gases produced by the roots of 1-week old (Panel a)**
737 **and 3-month old (Panel b) *M. pudica* plants.** In each case, a SPME fiber was exposed to the

738 headspace gases for 5 min and the fiber was then analyzed by DART-HRMS. The structures
739 shown are consistent with the observed HR elemental compositions and isotope data obtained.
740 Detected compounds were observed in their deprotonated forms. The mass measurements and
741 relative peak intensities associated with the data shown here are presented in Table S4.

742
743 **Figure 5. Differences in ion counts for some of the DART-HRMS detected compounds**
744 **emitted from untouched and touched roots (depicted in blue and red respectively).** The data
745 represent the average of three replicates of the actual DART-MS derived ion counts at each of
746 the nominal m/z values shown, and the ion counts reflect the amounts of the observed ions.
747 Mass-to-charge ratios are only shown for molecules whose touched and untouched ion counts
748 were different within experimental error. The errors were no more than $\pm 5\%$ in all cases. The
749 chemical species represented by the m/z values are the deprotonated forms of propanesulfenic
750 acid (m/z 91), 2-aminothiophenol (m/z 124), *S*-propyl propane-1-thiosulfinate (m/z 165), and
751 phenothiazine (m/z 198). The identity of the molecule represented by m/z value 239 is unknown.
752 The “Totals” bars represent the summation of total ion counts for all the indicated m/z values for
753 the unstimulated (blue) and stimulated (red) roots respectively.

754 **Figure 6. Representative cryo SEM (cSEM) micrographs of *M. pudica* seedling roots.** Panel
755 a: A segment of a root showing a high density of hair-like protuberances. Panel b: Expansion of
756 the boxed area shown in Panel a. Panel c: A segment of the same root shown in Panel a, that was
757 distal to that appearing in Panel a, in which the population of protuberances is sparse. Panel d: A
758 touched segment of a root shaft that was previously shown by light microscopy to have
759 protuberances. The protuberances are no longer present. Observed protuberances were 100—200
760 μm in length.

761 **Figure 7. Representative cryo SEM (cSEM)-electron dispersive spectroscopy (EDS)**
762 **micrograph of a section of a *M. pudica* seedling root densely populated with hairs that are**
763 **flattened (as opposed to turgid) under the high vacuum conditions of the analysis.** Panel a:
764 The hue of the image reflects the composite of the overlaid color-coded contributions of the
765 elements C, N, O, Mg, P, S, Cl^- , K^+ and Ca^{2+} . Panel b: X-ray maps of each of the color coded
766 elements contributing to the color composite shown in Panel a. Whereas in some cases, such as
767 for C, N and O, there is uniform elemental distribution, the concentrations of Cl^- and K^+ are

768 significant enough in some of the hairs that a general outline reflecting the topology of those
769 hairs in the cSEM image is revealed in their maps. Panel c: Elemental composition map sum
770 spectrum of the cSEM image shown in Panel a. The relative percentage contributions by weight
771 % are listed and show that besides C, N and O, K⁺ and Cl⁻ are present at the highest relative
772 concentrations.

773 **Figure 8. cSEM micrograph with EDS analysis of a section of a *M. pudica* root the left side**
774 **of which had been touched with a finger.** The root sample was flash frozen at liquid N₂
775 temperature immediately after an odor was detected. The cSEM micrograph (top panel) shows an
776 *M. pudica* root section which, prior to being touched, was shown by optical microscopy to be
777 heavily populated with glandular hairs on both sides. The micrograph shows that consistent with
778 previous observations, the hairs on the touched side of the root were no longer present. A few
779 flattened sacs can be seen on the right side. The EDS spectra for the indicated boxed inspection
780 fields shown in the micrograph are show in blue (bottom panel) with the observed elements
781 indicated (by relative weight %).

782
783 **Figure 9. Proposed mechanism for cysteine lyase-mediated degradation of djenkolic acid.**
784 In the first step, a Schiff base forms between djenkolic acid and the enzyme-derived pyridoxal
785 phosphate (PALP). Enzyme promoted proton abstraction from an α -carbon in the djenkolic acid-
786 PALP complex ultimately results in liberation of thioformaldehyde, cysteine and a pyridinium
787 ion, hydrolysis of which yields α -aminoacrylate. Further hydrolysis of this intermediate
788 furnishes ammonia and pyruvate.

789
790
791
792
793
794
795

796 **SUPPLEMENTARY FIGURES, TABLES AND VIDEOS**

797 **LEGENDS**

798 **Supplementary Figure 1**

799 **S1.** *M. pudica* seedlings germinated on agar showing the single tap root that emerges.

800

801 **Supplementary Figure S2.**

802 **S2.** Representative headspace gas analysis assembly used to sample the gases produced by *M.*
803 *pudica* seedlings.

804

805 **Supplementary Figure S3.**

806 **S3.** Glass growth chamber apparatus designed to sample and detect the headspaces gases of root
807 versus aerial parts of *M. pudica* seedlings independently. The experiment was conducted under
808 sterile conditions. Panel a: pyrex glass tube showing the plug of agar suspended in the middle;
809 Panel b: top down view of 3-day old *M. pudica* seedling deposited on the surface of the agar;
810 Panel c: side view of apparatus showing that the root of the seedling had emerged from the
811 bottom of the agar plug towards the water contained within the tube, without actually touching it.
812 The root headspace could be sampled by withdrawing the water using a syringe, and inserting a
813 PDMS SPME fiber which, after adsorption of headspace constituents, was analyzed by DART-
814 HRMS.

815

816 **Supplementary Figure S4.**

817 **S4.** Determination of odor emission in stimulated and unstimulated roots by a five-person
818 untrained human panel. Seedling roots were exposed to one of five stimuli (i.e. a human finger,
819 wood, glass, soil and stainless steel) as illustrated in Supplementary videos SV1 and SV2. For

820 the untouched, human touch, wood, glass, soil, and metal experiments, the percentage of
821 panelists with a positive response (indicating that they experienced an odor) was 45 ± 30 ; $85 \pm$
822 19 ; 35 ± 19 ; 10 ± 20 ; 100 and 35 ± 25 percent respectively. For each stimulus, each panelist was
823 exposed to five seedlings.

824

825 **Supplementary Figure S5**

826 **S5.** Typical results obtained for the GC-MS analysis of the headspace of *M. pudica* roots. Panel
827 a: gas chromatogram showing two components; Panel b: EI mass spectrum of the GC component
828 that appeared at a retention time of 1.36 min. The mass spectrum indicates that the compound is
829 carbon disulfide.

830

831 **Supplementary Figure S6**

832 **S6.** Light microscopy image of portion of an *M. pudica* seedling root at 6X magnification,
833 showing hair-like structures that appeared in clusters along the root shaft.

834

835 **Supplementary Figure S7**

836 **S7.** cSEM micrograph with EDS analysis of a section of a *M. pudica* root. The segment below
837 the diagonal line had been tapped once with a finger while that above the line had not. The root
838 sample was flash frozen at liquid N₂ temperature immediately after an odor was detected. The
839 cSEM micrograph (top panel) shows an *M. pudica* root section which, prior to being touched,
840 was observed by optical microscopy to be heavily populated with glandular hairs on both sides.
841 The micrograph shows that consistent with previous observations, the hairs on the touched side
842 of the root had collapsed. The EDS spectra for the indicated inspection fields (1, 2 and 3) are
843 shown in blue (bottom panel) with the observed elements indicated (by relative weight %).

844 **Supplementary Table S1**

845 **Table S1.** Mass measurements for the positive- and negative-ion mode DART-HRMS spectra of
846 the headspace of a 7-day old *M. pudica* seedling in the absence of an odor producing stimulus.

847

848 **Supplementary Table S2**

849 **Table S2.** Mass measurements for the negative-ion mode DART-HRMS spectra of the
850 headspace of untouched root and aerial parts of a 7-day old *M. pudica* seedling.

851

852 **Supplementary Video 1**

853 **SV1.** Demonstration of how to elicit emission of odor compounds from an *M. pudica* root by
854 exposure of the root to human skin.

855

856 **Supplementary Video 2**

857 **SV2.** Demonstration of how to elicit emission of odor compounds from an *M. pudica* root by
858 exposure of the root to soil.

859

860 **ACKNOWLEDGEMENTS**

861 The authors are thankful to Marek Domin for helpful discussions regarding SPME experiments,
862 to Justine Giffen for filming the videos and assisting with germination of the seedlings for the
863 odor panel experiments, and to Donna Guarrera for assistance with the X-ray fluorescence
864 measurements.

865

866

867

868

869

870 **LITERATURE CITED**

- 871 **Agúndez M, Fonfría JP, Cernicharo J, Pardo JR, Guélin M** (2008) Detection of circumstellar CH₂, CHCN,
 872 CH₂CN, CH₃CCH and H₂CS. *Astron. Astrophys.* **479**: 493-501
- 873 **Bisio A, Corallo A, Gastaldo P, Romussi G, Ciarallo G, Fontana N, De Tommasi N, Profumo P** (1999)
 874 Glandular hairs and secreted material in *Salvia blepharophylla* Brandegees ex Epling grown in
 875 Italy. *Ann. Bot.* **83**: 441-452
- 876 **Block E** (1992) The organosulfur chemistry of the genus *Allium* – Implications for the organic chemistry
 877 of sulfur. *Angew. Chem. Int. Ed. Engl.* **31**: 1135-1178
- 878 **Block E** (2011) Challenges and artifact concerns in analysis of volatile sulfur compounds. *In* Volatile
 879 Sulfur Compounds in Food, Vol 1068. American Chemical Society, pp 35-63
- 880 **Block E, Dane AJ, Cody RB** (2011) Crushing garlic and slicing onions: Detection of sulfenic acids and other
 881 reactive organosulfur intermediates from garlic and other *Alliums* using direct analysis in real-
 882 time mass spectrometry (DART-MS). *Phosphorus Sulfur* **186**: 1085-1093
- 883 **Block E, Dane AJ, Thomas S, Cody RB** (2010) Applications of direct analysis in real time mass
 884 spectrometry (DART-MS) in *Allium* chemistry. 2-Propenesulfenic and 2-propenesulfinic acids,
 885 diallyl trisulfane S-oxide, and other reactive sulfur compounds from crushed garlic and other
 886 *Alliums*. *J. Agric. Food Chem.* **58**: 4617-4625
- 887 **Braam J** (2005) In touch: plant responses to mechanical stimuli. *New Phytol.* **165**: 373-389
- 888 **Cody RB, Laramée JA, Durst HD** (2005) Versatile new ion source for the analysis of materials in open air
 889 under ambient conditions. *Anal. Chem.* **77**: 2297-2302
- 890 **Crespo E, Hordijk CA, de Graaf RM, Samudrala D, Cristescu SM, Harren FJM, van Dam NM** (2012) On-
 891 line detection of root-induced volatiles in *Brassica nigra* plants infested with *Delia radicum* L.
 892 root fly larvae. *Phytochemistry* **84**: 68-77
- 893 **Danner H, Samudrala D, Cristescu S, Van Dam N** (2012) Tracing hidden herbivores: Time-resolved non-
 894 invasive analysis of belowground volatiles by proton-transfer-reaction mass spectrometry (PTR-
 895 MS). *J. Chem. Ecol.* **38**: 785-794
- 896 **Darwin C** (1880) *The Power of Movement in Plants*. William Clowes and Sons Ltd., London
- 897 **Darwin C** (1893) *Insectivorous Plants*. John Murray, London
- 898 **De-la-Peña C, Badri D, Loyola-Vargas V** (2012) Plant root secretions and their interactions with
 899 neighbors. *In* JM Vivanco, F Baluška, eds, *Secretions and Exudates in Biological Systems*, Vol 12.
 900 Springer Berlin Heidelberg, pp 1-26
- 901 **Domin MC, Codyl, RB**, Ed (2014) *Ambient Ionization Mass Spectrometry*. Royal Society of Chemistry,
 902 London
- 903 **Eisner T** (1981) Leaf folding in a sensitive plant: A defensive thorn-exposure mechanism? *Proc. Natl.*
 904 *Acad. Sci. USA.* **78**: 402-404
- 905 **Farkas P, Hradský P, Kováč M** (1992) Novel flavour components identified in the steam distillate of
 906 onion (*Allium cepa* L.). *Z. Lebensm. Unters. For.* **195**: 459-462
- 907 **Feng Z, Hartel P** (1996) Factors affecting production of COS and CS₂ in *Leucaena* and *Mimosa* species.
 908 *Plant Soil* **178**: 215-222
- 909 **Fromm J, Eschrich W** (1988) Transport processes in stimulated and non-stimulated leaves of *Mimosa*
 910 *pudica*. *Trees* **2**: 18-24
- 911 **Haines B, Black M, Bayer C** (1989) Sulfur emissions from roots of the rain forest tree *Stryphnodendron*
 912 *excelsum*. *Biogenic Sulfur in the Environment* **393**: 58-69
- 913 **Haines BL** (1991) Proceedings of the International Workshop on Modern Techniques in Soil Ecology
 914 Relevant to Organic Matter Breakdown, Nutrient Cycling and Soil Biological Processes:
 915 Identification and quantification of sulfur gases emitted from soils, leaf litter and live plant parts.
 916 *Agric. Ecosystems Environ.* **34**: 473-477

- 917 **Hartel PG, Haines BL** (1992) Effects of potential plant CS₂ emissions on bacterial growth in the
918 rhizosphere. *Soil Biol. Biochem.* **24**: 219-224
- 919 **Hartel PG, Reeder RE** (1993) Effects of drought and root injury on plant-generated CS₂ emissions in soil.
920 *Plant Soil* **148**: 271-276
- 921 **Head GC** (1964) A Study of 'exudation' from the root hairs of apple roots by time-lapse cine-
922 photomicrography. *Ann. Bot.* **28**: 495-498
- 923 **Holm LGP, D. L.; Pancho, J. V.; Herberger, J. P.** (1977) The worlds worst weeds. Distribution and biology.
924 University Press of Hawaii, Honolulu, Hawaii, USA
- 925 **Howard RA** (1988) Flora of the Lesser Antilles, Leeward and Winward Islands. Dicotyledoneae, Part 1,
926 Vol 4. Arnold Arboretum, Harvard University, Jamaica Plain, MA
- 927 **Jacox ME, Milligan DE** (1975) Matrix isolation study of the infrared spectrum of thioformaldehyde. *J.*
928 *Mol. Spectrosc.* **58**: 142-157
- 929 **Kellogg DW, Taylor TN, Krings M** (2002) Effectiveness in defense against phytophagous arthropods of
930 the cassabanana (*Sicana odorifera*) glandular trichomes. *Entomol. Exp. Appl.* **103**: 187-189
- 931 **Krings M, Kellogg DW, Kerp H, Taylor TN** (2003) Trichomes of the seed fern *Blanzyspteris praedentata*:
932 implications for plant-insect interactions in the Late Carboniferous. *Bot. J. Linn. Soc.* **141**: 133-
933 149
- 934 **Krings M, Taylor, Thomas N., Kellogg, Derek W.** (2002) Touch-sensitive glandular trichomes: a mode of
935 defence against herbivorous arthropods in the Carboniferous. *Evol. Ecol. Res.* **4**: 779-786
- 936 **Kubec R, Cody RB, Dane AJ, Musah RA, Schraml J, Vattekkatte A, Block E** (2010) Applications of direct
937 analysis in real time-mass spectrometry (DART-MS) in *Allium* chemistry. (Z)-butanethial S-oxide
938 and 1-butenyl thiosulfinates and their S-(E)-1-butenylcysteine S-oxide precursor from *Allium*
939 *siculum*. *J. Agric. Food Chem.* **58**: 1121-1128
- 940 **Leonardos G, Kendall D, Barnard N** (1969) Odor Threshold Determinations of 53 Odorant Chemicals. *J.*
941 *Air Pollut. Control Assoc.* **19**: 91-95
- 942 **Massa GD, Gilroy S** (2003) Touch modulates gravity sensing to regulate the growth of primary roots of
943 *Arabidopsis thaliana*. *Plant J.* **33**: 435-445
- 944 **Netzly DH, Butler LG** (1986) Roots of *Sorghum* exude hydrophobic droplets containing biologically active
945 components. *Crop Sci.* **26**: 775-778
- 946 **Okada K, Shimura Y** (1990) Reversible root tip rotation in *Arabidopsis* seedlings induced by obstacle-
947 touching stimulus. *Science* **250**: 274-276
- 948 **Penn RE, Block E, Revelle LK** (1978) Flash vacuum pyrolysis studies. 5. Methanesulfenic acid. *J. Am.*
949 *Chem. Soc.* **100**: 3622-3623
- 950 **Pickard BG** (1973) Action potentials in higher plants. *Bot. Rev.* **39**: 172-201
- 951 **Piluk J, Hartel P, Haines B** (1998) Production of carbon disulfide (CS₂) from L-djenkolic acid in the roots
952 of *Mimosa pudica* L. *Plant Soil* **200**: 27-32
- 953 **Piluk J, Hartel PG, Haines BL, Giannasi DE** (2001) Association of carbon disulfide with plants in the family
954 *Fabaceae*. *J. Chem. Ecol.* **27**: 1525-1534
- 955 **Samudrala D, Brown PA, Mandon J, Cristescu SM, Harren FJM** (2015) Optimization and sensitive
956 detection of sulfur compounds emitted from plants using proton transfer reaction mass
957 spectrometry. *Int. J. Mass Spectrom.* **386**: 6-14
- 958 **Simons PJ** (1981) The role of electricity in plant movements *New Phytol.* **87**: 11-37
- 959 **Solouki B, Rosmus P, Bock H** (1976) Unstable intermediates. 4. Thioformaldehyde. *J. Am. Chem. Soc.* **98**:
960 6054-6055
- 961 **Song K, Yeom E, Lee SJ** (2014) Real-time imaging of pulvinus bending in *Mimosa pudica*. *Scientific*
962 *Reports* **4**: 6466
- 963 **Suzuki E, Yamazaki M, Shimizu K** (2007) Infrared spectra of monomeric thioformaldehyde in Ar, N₂ and
964 Xe matrices. *Vib. Spectrosc.* **43**: 269-273

965 **Tissier A** (2012) Glandular trichomes: what comes after expressed sequence tags? *Plant J.* **70**: 51-68
966 **Torres M, Safarik I, Clement A, Strausz OP** (1982) The generation and vibrational spectrum of matrix
967 isolated thioformaldehyde and dideuterothioformaldehyde. *Can. J. Chem.* **60**: 1187-1191
968 **van Dam NM, Samudrala D, Harren FJM, Cristescu SM** (2012) Real-time analysis of sulfur-containing
969 volatiles in Brassica plants infested with root-feeding *Delia radicum* larvae using proton-transfer
970 reaction mass spectrometry. *AoB Plants* **2012**
971 **Visnovitz T, Világi I, Varró P, Kristóf Z** (2007) Mechanoreceptor cells on the tertiary pulvini of *Mimosa*
972 *pubica* L. *Plant Signal. Behav.* **2**: 462-466
973 **Volkov AG, Foster JC, Ashby TA, Walker RK, Johnson JA, Markin VS** (2010) *Mimosa pudica*: Electrical
974 and mechanical stimulation of plant movements. *Plant Cell Environ.* **33**: 163-173
975 **Volkov AG, Foster JC, Baker KD, Markin VS** (2010) Mechanical and electrical anisotropy in *Mimosa*
976 *pubica* pulvini. *Plant Signal. Behav.* **5**: 1211-1221
977 **Volkov AG, Reedus J, Mitchell CM, Tuckett C, Volkova MI, Markin VS, Chua L** (2014) Memory elements
978 in the electrical network of *Mimosa pudica* L. *Plant Signal. Behav.* **9**: e982029
979 **Watanabe O, Suzuki E, Watari F** (1991) Photolysis of thietane and thietane-d6 in argon matrix: infrared
980 spectra of matrix-isolated thioformaldehyde and thioformaldehyde-d2. *Bull. Chem. Soc. Jpn.* **64**:
981 1389-1391

982

983

984

985

986

987

988

989

990

991

992

993

994

995

996

997

998

999

1000

FIGURE 1

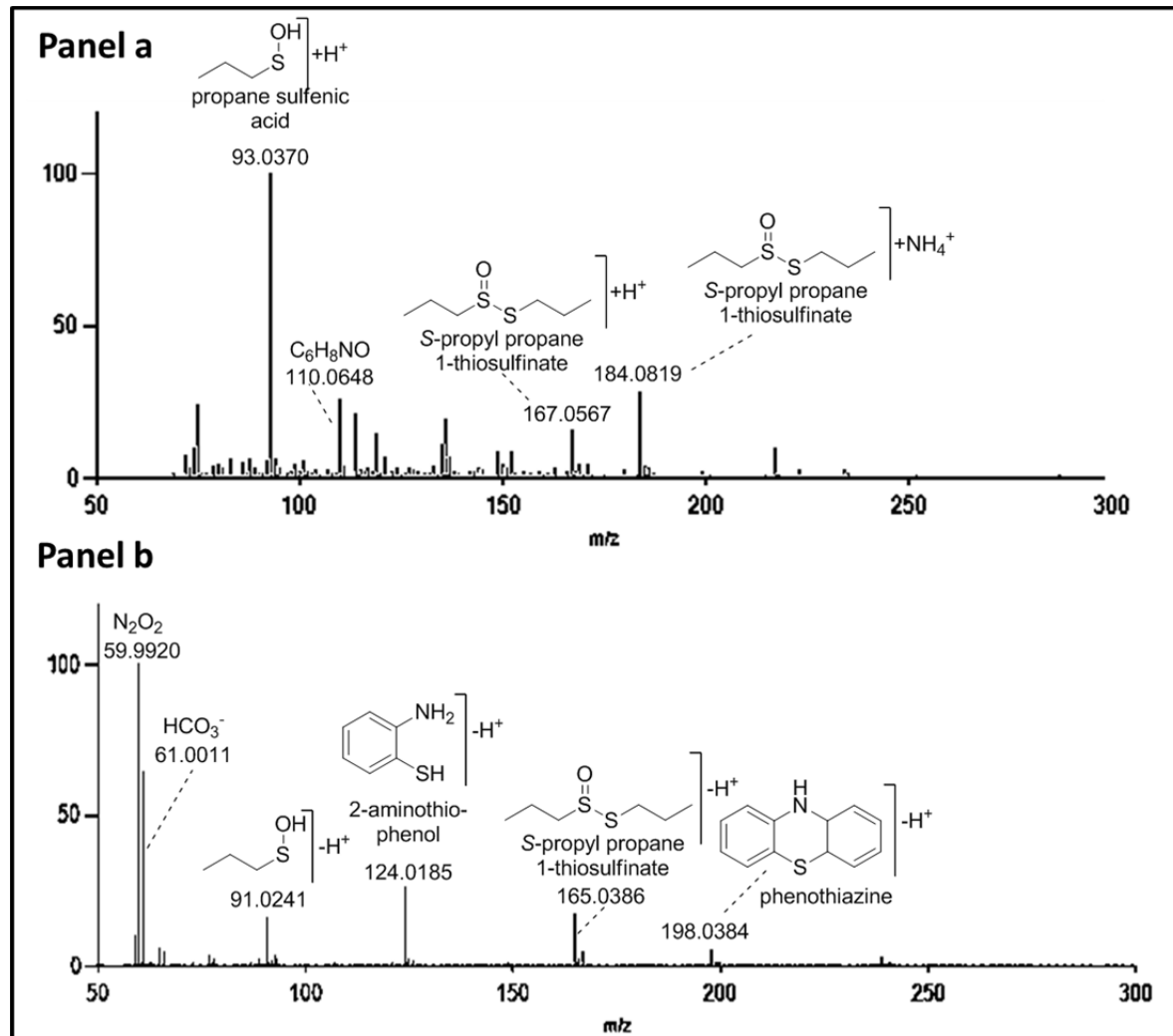


Figure 1. Typically observed DART-HRMS positive- and negative-ion mode spectra of the headspace of 7-day old *M. pudica* seedlings in the absence of an odor producing stimulus. In each case, a SPME fiber was exposed to the headspace for 5 min, and the fiber was then analyzed by DART-HRMS. The structures shown are consistent with the observed HR elemental compositions and isotope data obtained, as well as the results of comparisons of the fragmentation patterns observed for standards under in-source CID conditions, to that of the headspace samples also obtained under in-source CID conditions. Detected compounds were observed in their protonated or ammoniated forms. The mass measurements and relative peak abundances associated with the data shown here are presented in Table S1.

FIGURE 2

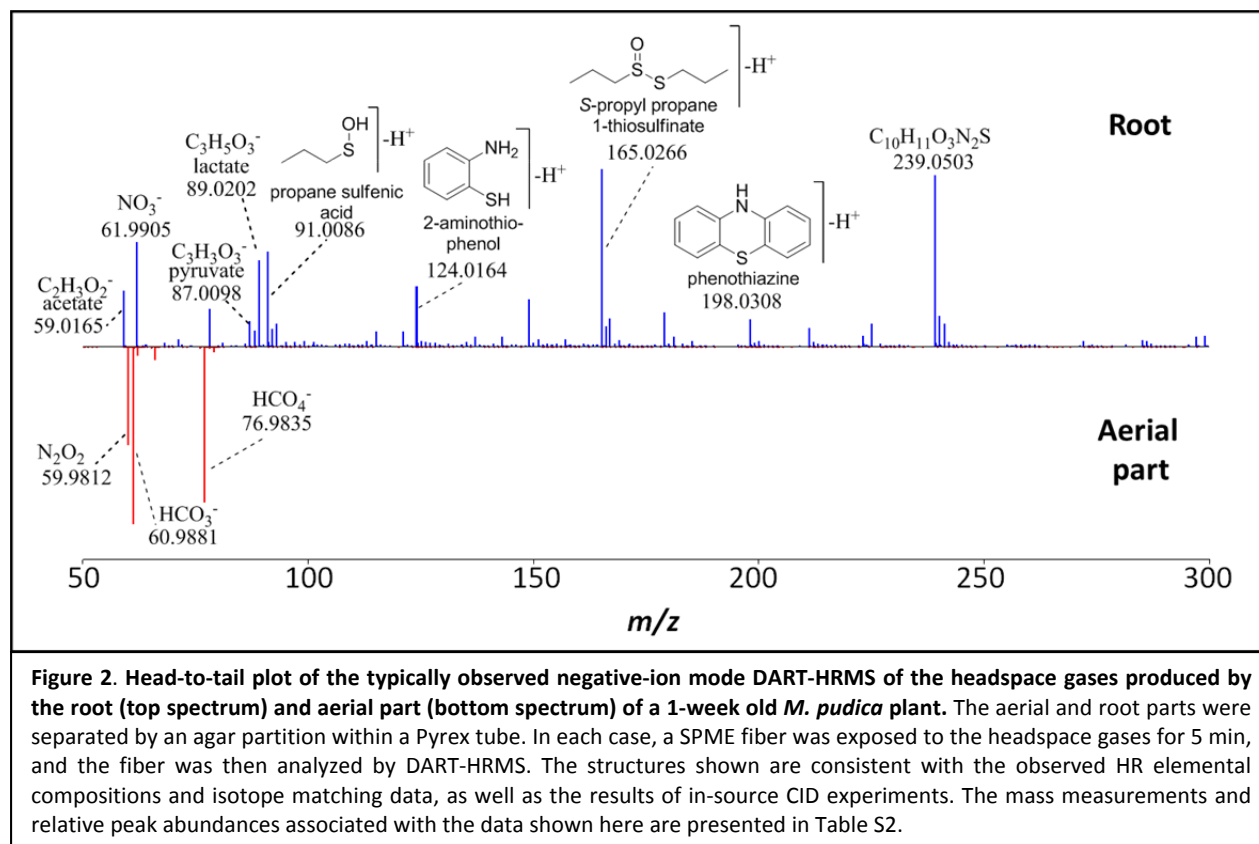


FIGURE 3

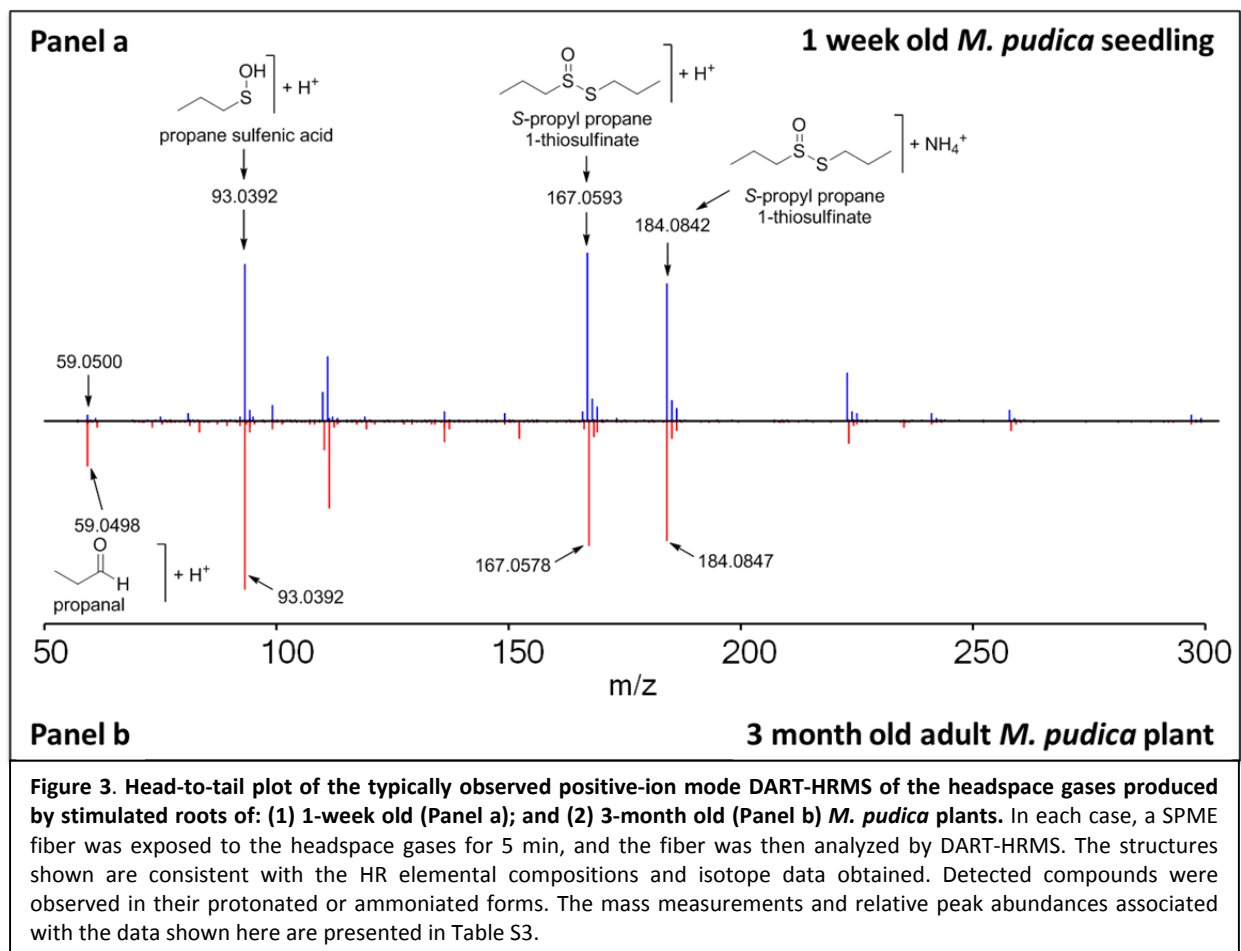


FIGURE 4

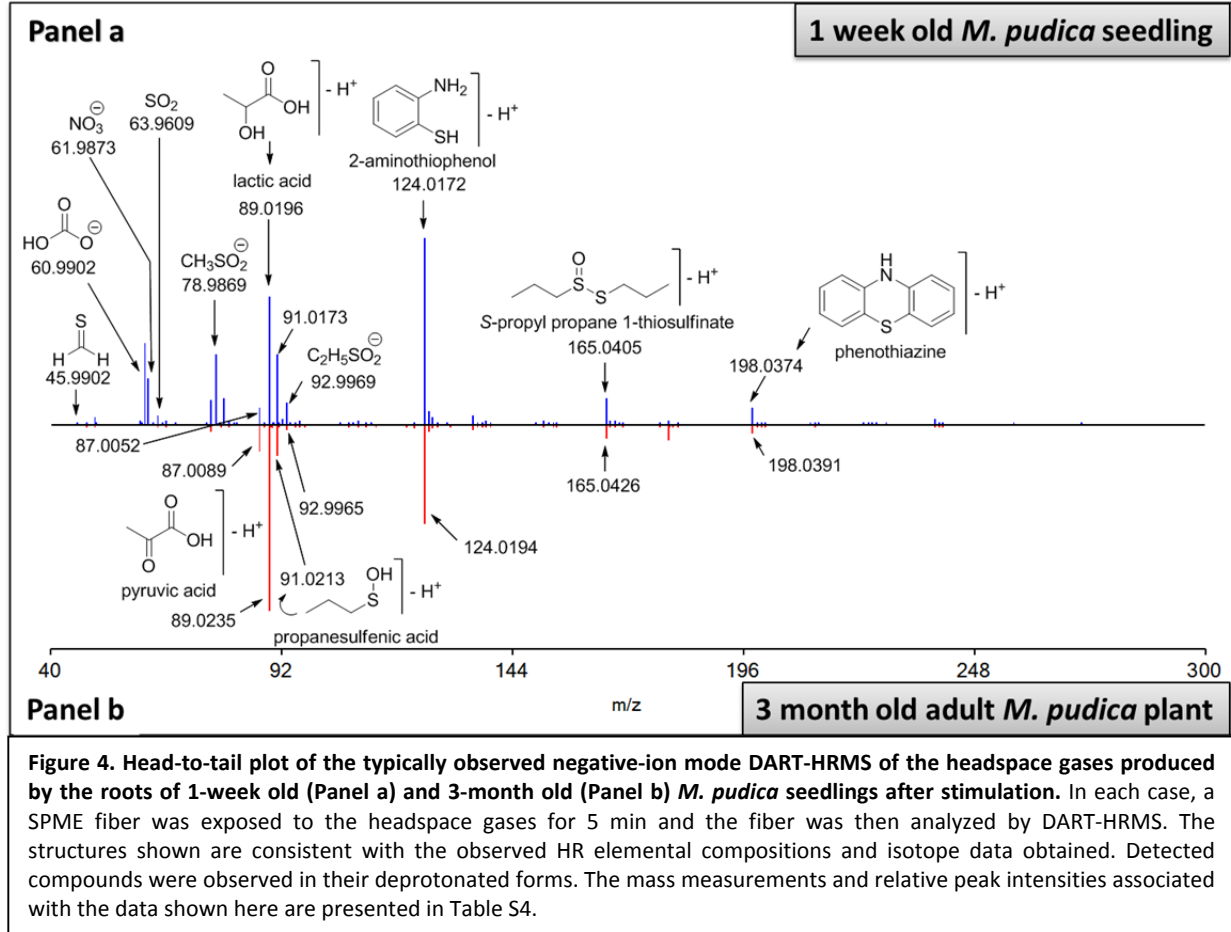


FIGURE 5

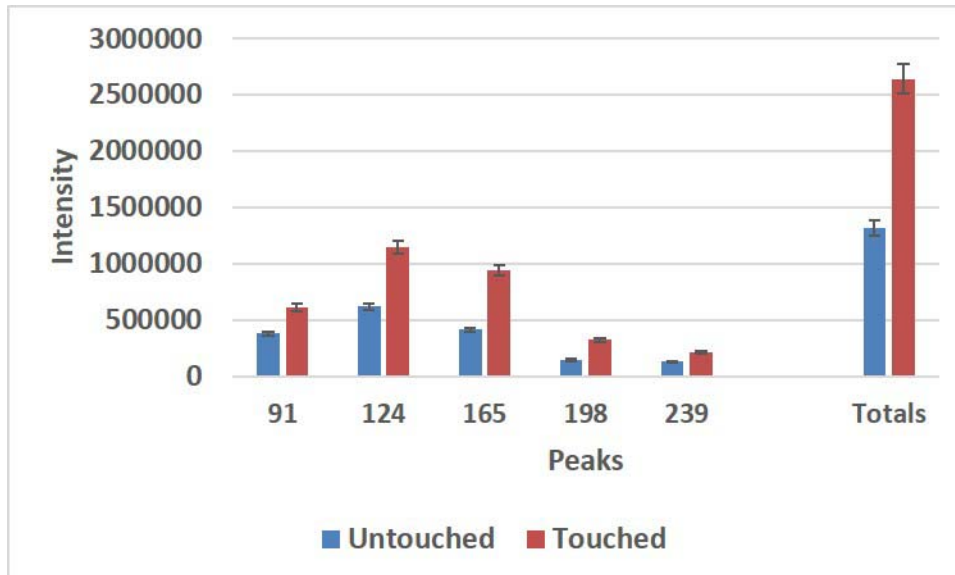


Figure 5. Differences in ion counts for some of the DART-HRMS detected compounds emitted from untouched and touched roots (depicted in blue and red respectively). The data represent the average of three replicates of the actual DART-HRMS derived ion counts at each of the m/z values shown, and the ion counts reflect the amounts of the observed ions. Mass-to-charge ratios are only shown for molecules whose touched and untouched ion counts were different within experimental error. The errors were no more than $\pm 5\%$ in all cases. The chemical species represented by the nominal m/z values are the deprotonated forms of propanesulfenic acid (m/z 91), 2-aminothiophenol (m/z 124), *S*-propyl propane-1-thiosulfinate (m/z 165), and phenothiazine (m/z 198). The identity of the molecule represented by m/z value 239 is unknown. The "Totals" bars represent the summation of total ion counts for all the indicated m/z values for the unstimulated (blue) and stimulated (red) roots respectively.

FIGURE 6

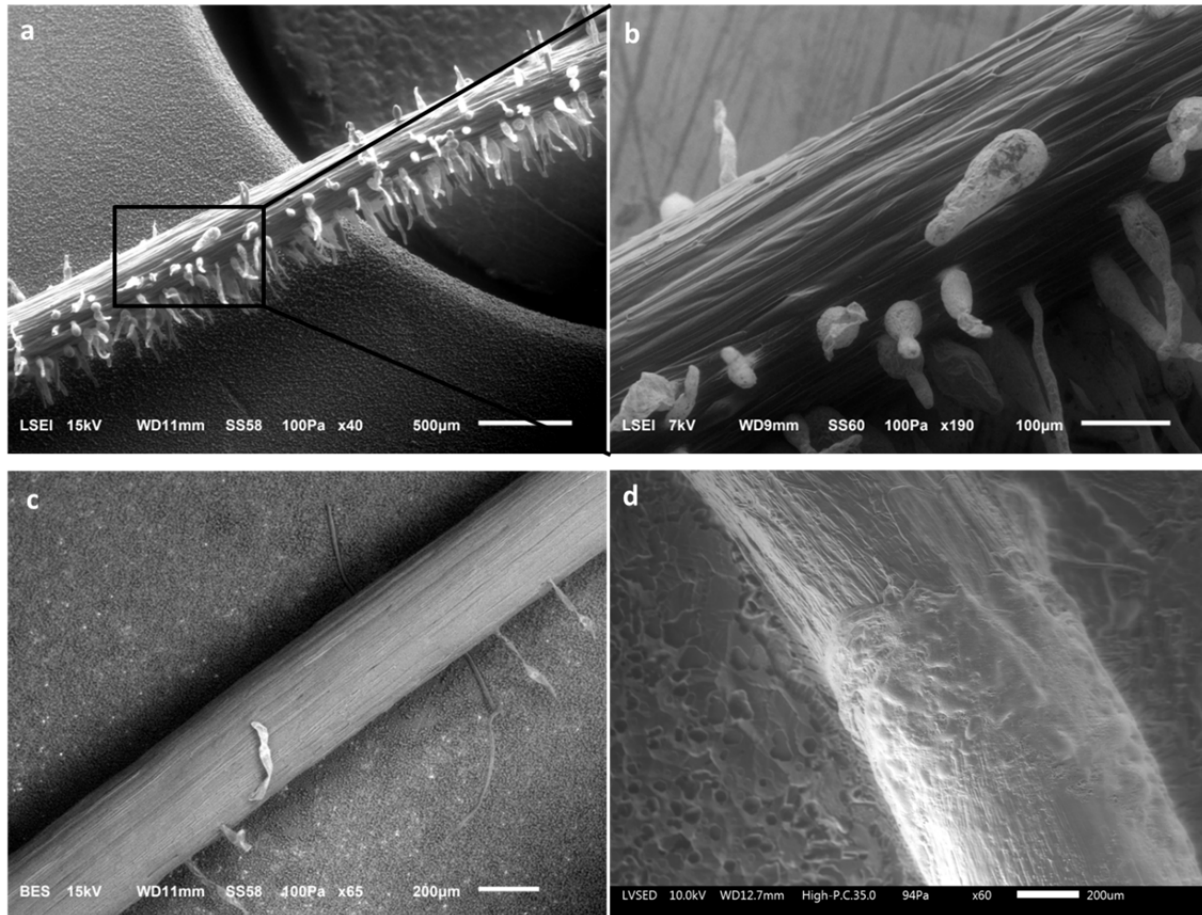


Figure 6. Representative cryo SEM (cSEM) micrographs of *M. pudica* seedling roots. Panel a: A segment of a root showing a high density of hair-like protuberances. Panel b: Expansion of the boxed area shown in Panel a. Panel c: A segment of the same root shown in Panel a, that was distal to that appearing in Panel a, in which the population of protuberances is sparse. Panel d: A touched segment of a root shaft that was previously shown by light microscopy to have protuberances. The protuberances had collapsed. Observed protuberances were 100–200 µm in length.

FIGURE 7

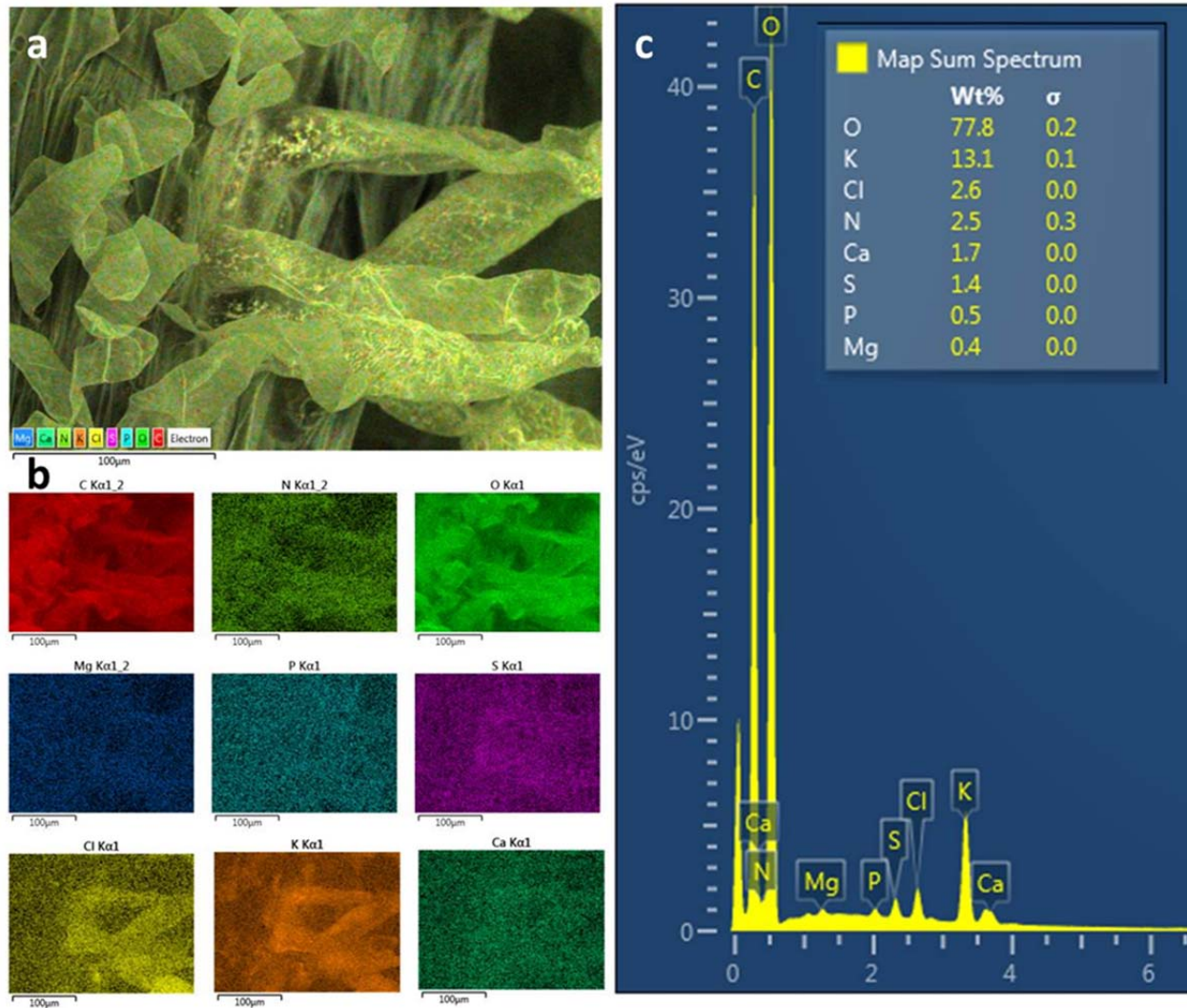


Figure 7. Representative cryo SEM (cSEM)-electron dispersive spectroscopy (EDS) micrograph of a section of a *M. pudica* seedling root densely populated with hairs that are flattened (as opposed to turgid) under the high vacuum conditions of the analysis. Panel a: The hue of the image reflects the composite of the overlaid color-coded contributions of the elements C, N, O, Mg, P, S, Cl⁻, K⁺ and Ca²⁺. Panel b: X-ray maps of each of the color coded elements contributing to the color composite shown in Panel a. Whereas in some cases, such as for C, N and O, there is uniform elemental distribution, the concentrations of Cl⁻ and K⁺ are significant enough in some of the hairs that a general outline reflecting the topology of those hairs in the cSEM image is revealed in their maps. Panel c: Elemental composition map sum spectrum of the cSEM image shown in Panel a. The relative percentage contributions by weight % are listed and show that besides C, N and O, K⁺ and Cl⁻ are present at the highest relative concentrations.

FIGURE 8

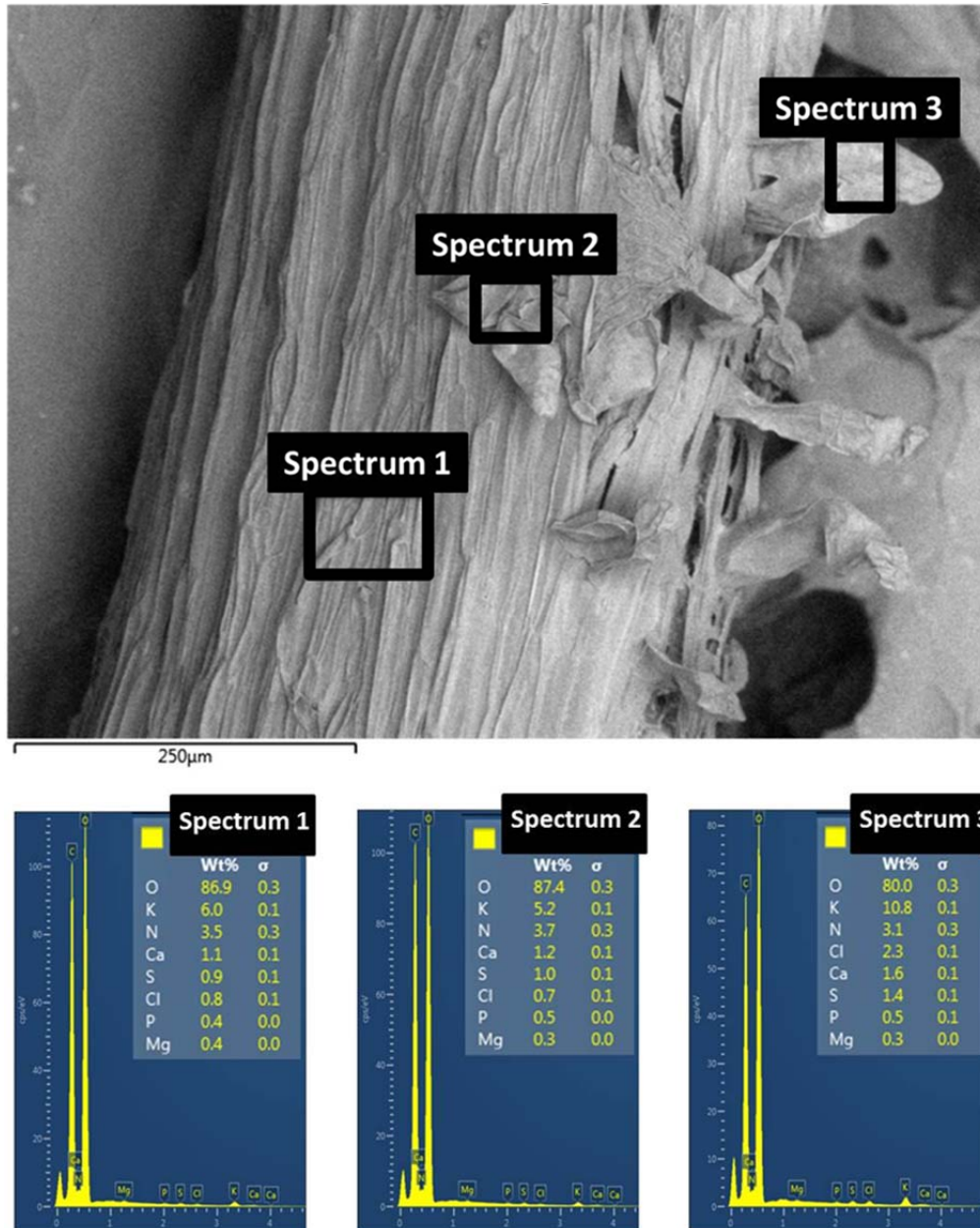


Figure 8. cSEM micrograph with EDS analysis of a section of a *M. pudica* root the left side of which had been touched with a finger. The root sample was flash frozen at liquid N₂ temperature immediately after an odor was detected. The cSEM micrograph (top panel) shows an *M. pudica* root section which, prior to being touched, was shown by optical microscopy to be heavily populated with glandular hairs on both sides. The micrograph shows that consistent with previous observations, the hairs on the touched side of the root had collapsed. A few flattened sacs can be seen on the right side. The EDS spectra for the indicated boxed inspection fields indicated in the micrograph are shown in blue (bottom panel) with the observed elements indicated (by relative weight %).

FIGURE 9

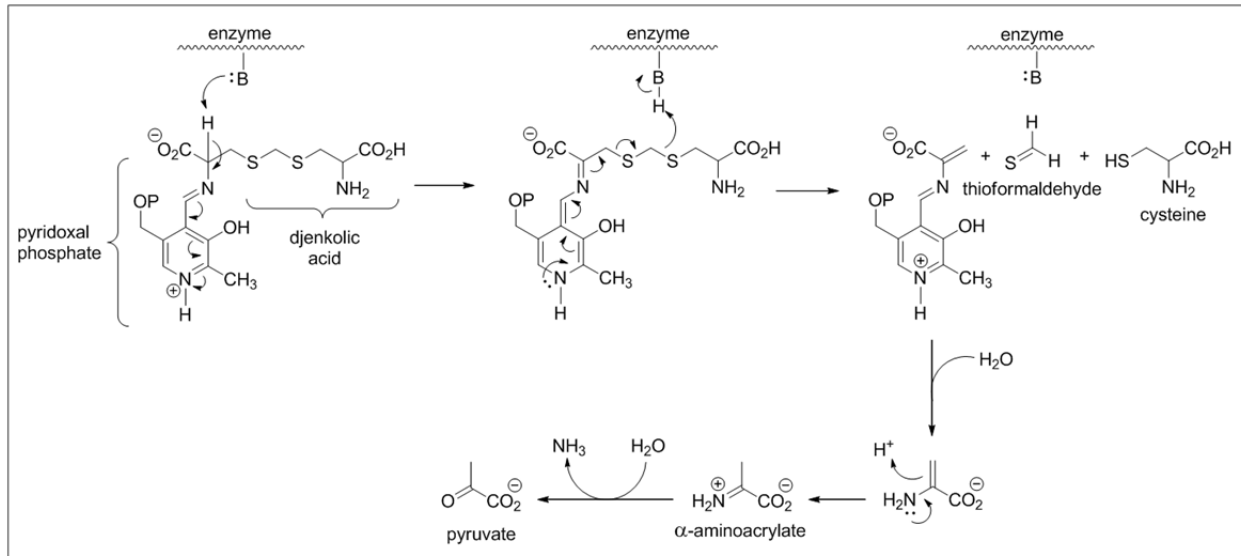


Figure 9. Proposed mechanism for cysteine lyase-mediated degradation of djenkolic acid. In the first step, a Schiff base forms between djenkolic acid and the enzyme-derived pyridoxal phosphate (PALP). Enzyme promoted proton abstraction from an α -carbon in the djenkolic acid-PALP complex ultimately results in liberation of thioformaldehyde, cysteine and a pyridinium ion, hydrolysis of which yields α -aminoacrylate. Further hydrolysis of this intermediate furnishes ammonia and pyruvate.

Parsed Citations

Agúndez M, Fonfría JP, Cernicharo J, Pardo JR, Guélin M (2008) Detection of circumstellar CH₂, CHCN, CH₂CN, CH₃CCH and H₂CS. *Astron. Astrophys.* 479: 493-501

Pubmed: [Author and Title](#)

CrossRef: [Author and Title](#)

Google Scholar: [Author Only](#) [Title Only](#) [Author and Title](#)

Bisio A, Corallo A, Gastaldo P, Romussi G, Ciarallo G, Fontana N, De Tommasi N, Profumo P (1999) Glandular hairs and secreted material in *Salvia blepharophylla* Brandegeee ex Epling grown in Italy. *Ann. Bot.* 83: 441-452

Pubmed: [Author and Title](#)

CrossRef: [Author and Title](#)

Google Scholar: [Author Only](#) [Title Only](#) [Author and Title](#)

Block E (1992) The organosulfur chemistry of the genus *Allium* - Implications for the organic chemistry of sulfur. *Angew. Chem. Int. Ed. Engl.* 31: 1135-1178

Pubmed: [Author and Title](#)

CrossRef: [Author and Title](#)

Google Scholar: [Author Only](#) [Title Only](#) [Author and Title](#)

Block E (2011) Challenges and artifact concerns in analysis of volatile sulfur compounds. In *Volatile Sulfur Compounds in Food, Vol 1068. American Chemical Society*, pp 35-63

Pubmed: [Author and Title](#)

CrossRef: [Author and Title](#)

Google Scholar: [Author Only](#) [Title Only](#) [Author and Title](#)

Block E, Dane AJ, Cody RB (2011) Crushing garlic and slicing onions: Detection of sulfenic acids and other reactive organosulfur intermediates from garlic and other *Alliums* using direct analysis in real-time mass spectrometry (DART-MS). *Phosphorus Sulfur* 186: 1085-1093

Pubmed: [Author and Title](#)

CrossRef: [Author and Title](#)

Google Scholar: [Author Only](#) [Title Only](#) [Author and Title](#)

Block E, Dane AJ, Thomas S, Cody RB (2010) Applications of direct analysis in real time mass spectrometry (DART-MS) in *Allium* chemistry. 2-Propenesulfenic and 2-propenesulfinic acids, diallyl trisulfane S-oxide, and other reactive sulfur compounds from crushed garlic and other *Alliums*. *J. Agric. Food Chem.* 58: 4617-4625

Pubmed: [Author and Title](#)

CrossRef: [Author and Title](#)

Google Scholar: [Author Only](#) [Title Only](#) [Author and Title](#)

Braam J (2005) In touch: plant responses to mechanical stimuli. *New Phytol.* 165: 373-389

Pubmed: [Author and Title](#)

CrossRef: [Author and Title](#)

Google Scholar: [Author Only](#) [Title Only](#) [Author and Title](#)

Cody RB, Laramée JA, Durst HD (2005) Versatile new ion source for the analysis of materials in open air under ambient conditions. *Anal. Chem.* 77: 2297-2302

Pubmed: [Author and Title](#)

CrossRef: [Author and Title](#)

Google Scholar: [Author Only](#) [Title Only](#) [Author and Title](#)

Crespo E, Hordijk CA, de Graaf RM, Samudrala D, Cristescu SM, Harren FJM, van Dam NM (2012) On-line detection of root-induced volatiles in *Brassica nigra* plants infested with *Delia radicum* L. root fly larvae. *Phytochemistry* 84: 68-77

Pubmed: [Author and Title](#)

CrossRef: [Author and Title](#)

Google Scholar: [Author Only](#) [Title Only](#) [Author and Title](#)

Danner H, Samudrala D, Cristescu S, Van Dam N (2012) Tracing hidden herbivores: Time-resolved non-invasive analysis of belowground volatiles by proton-transfer-reaction mass spectrometry (PTR-MS). *J. Chem. Ecol.* 38: 785-794

Pubmed: [Author and Title](#)

CrossRef: [Author and Title](#)

Google Scholar: [Author Only](#) [Title Only](#) [Author and Title](#)

Darwin C (1880) *The Power of Movement in Plants*. William Clowes and Sons Ltd., London

Pubmed: [Author and Title](#)

CrossRef: [Author and Title](#)

Google Scholar: [Author Only](#) [Title Only](#) [Author and Title](#)

Darwin C (1893) *Insectivorous Plants*. John Murray, London

Pubmed: [Author and Title](#)

CrossRef: [Author and Title](#)

Google Scholar: [Author Only](#) [Title Only](#) [Author and Title](#)

De-la-Peña C, Badri D, Loyola-Vargas V (2012) Plant root secretions and their interactions with neighbors. In JM Vivanco, F Baluška, eds, *Secretions and Exudates in Biological Systems, Vol 12*. Springer Berlin Heidelberg, pp 1-26

Pubmed: [Author and Title](#)

CrossRef: [Author and Title](#)

Google Scholar: [Author Only](#) [Title Only](#) [Author and Title](#)

Domin MC, Codyl, RB, Ed (2014) *Ambient Ionization Mass Spectrometry*. Royal Society of Chemistry, London

Pubmed: [Author and Title](#)
CrossRef: [Author and Title](#)
Google Scholar: [Author Only](#) [Title Only](#) [Author and Title](#)

Eisner T (1981) Leaf folding in a sensitive plant: A defensive thorn-exposure mechanism? Proc. Natl. Acad. Sci. USA 78: 402-404

Pubmed: [Author and Title](#)
CrossRef: [Author and Title](#)
Google Scholar: [Author Only](#) [Title Only](#) [Author and Title](#)

Farkas P, Hradský P, Kováč M (1992) Novel flavour components identified in the steam distillate of onion (*Allium cepa* L.). Z. Lebensm. Unters. For. 195: 459-462

Pubmed: [Author and Title](#)
CrossRef: [Author and Title](#)
Google Scholar: [Author Only](#) [Title Only](#) [Author and Title](#)

Feng Z, Hartel P (1996) Factors affecting production of COS and CS₂ in *Leucaena* and *Mimosa* species. Plant Soil 178: 215-222

Pubmed: [Author and Title](#)
CrossRef: [Author and Title](#)
Google Scholar: [Author Only](#) [Title Only](#) [Author and Title](#)

Fromm J, Eschrich W (1988) Transport processes in stimulated and non-stimulated leaves of *Mimosa pudica*. Trees 2: 18-24

Pubmed: [Author and Title](#)
CrossRef: [Author and Title](#)
Google Scholar: [Author Only](#) [Title Only](#) [Author and Title](#)

Haines B, Black M, Bayer C (1989) Sulfur emissions from roots of the rain forest tree *Stryphnodendron excelsum*. Biogenic Sulfur in the Environment 393: 58-69

Pubmed: [Author and Title](#)
CrossRef: [Author and Title](#)
Google Scholar: [Author Only](#) [Title Only](#) [Author and Title](#)

Haines BL (1991) Proceedings of the International Workshop on Modern Techniques in Soil Ecology Relevant to Organic Matter Breakdown, Nutrient Cycling and Soil Biological Processes: Identification and quantification of sulfur gases emitted from soils, leaf litter and live plant parts. Agric. Ecosystems Environ. 34: 473-477

Pubmed: [Author and Title](#)
CrossRef: [Author and Title](#)
Google Scholar: [Author Only](#) [Title Only](#) [Author and Title](#)

Hartel PG, Haines BL (1992) Effects of potential plant CS₂ emissions on bacterial growth in the rhizosphere. Soil Biol. Biochem. 24: 219-224

Pubmed: [Author and Title](#)
CrossRef: [Author and Title](#)
Google Scholar: [Author Only](#) [Title Only](#) [Author and Title](#)

Hartel PG, Reeder RE (1993) Effects of drought and root injury on plant-generated CS₂ emissions in soil. Plant Soil 148: 271-276

Pubmed: [Author and Title](#)
CrossRef: [Author and Title](#)
Google Scholar: [Author Only](#) [Title Only](#) [Author and Title](#)

Head GC (1964) A Study of 'exudation' from the root hairs of apple roots by time-lapse cine-photomicrography. Ann. Bot. 28: 495-498

Pubmed: [Author and Title](#)
CrossRef: [Author and Title](#)
Google Scholar: [Author Only](#) [Title Only](#) [Author and Title](#)

Holm LGP, D. L.; Pancho, J. V.; Herberger, J. P. (1977) The worlds worst weeds. Distribution and biology. University Press of Hawaii, Honolulu, Hawaii, USA

Pubmed: [Author and Title](#)
CrossRef: [Author and Title](#)
Google Scholar: [Author Only](#) [Title Only](#) [Author and Title](#)

Howard RA (1988) Flora of the Lesser Antilles, Leeward and Windward Islands. Dicotyledoneae, Part 1, Vol 4. Arnold Arboretum, Harvard University, Jamaica Plain, MA

Pubmed: [Author and Title](#)
CrossRef: [Author and Title](#)
Google Scholar: [Author Only](#) [Title Only](#) [Author and Title](#)

Jacox ME, Milligan DE (1975) Matrix isolation study of the infrared spectrum of thioformaldehyde. J. Mol. Spectrosc. 58: 142-157

Pubmed: [Author and Title](#)
CrossRef: [Author and Title](#)
Google Scholar: [Author Only](#) [Title Only](#) [Author and Title](#)

Kellogg DW, Taylor TN, Krings M (2002) Effectiveness in defense against phytophagous arthropods of the cassabanana (*Sicana odorifera*) glandular trichomes. Entomol. Exp. Appl. 103: 187-189

Pubmed: [Author and Title](#)
CrossRef: [Author and Title](#)
Google Scholar: [Author Only](#) [Title Only](#) [Author and Title](#)

Krings M, Kellogg DW, Kerp H, Taylor TN (2003) Trichomes of the seed fern *Blanziopteris praedentata*: implications for plant-insect interactions in the Late Carboniferous. Bot. J. Linn. Soc. 141: 133-149

Pubmed: [Author and Title](#) Downloaded from www.plantphysiol.org on January 27, 2016 - Published by www.plant.org
Copyright © 2015 American Society of Plant Biologists. All rights reserved.

CrossRef: [Author and Title](#)
Google Scholar: [Author Only](#) [Title Only](#) [Author and Title](#)

Krings M, Taylor, Thomas N., Kellogg, Derek W. (2002) Touch-sensitive glandular trichomes: a mode of defence against herbivorous arthropods in the Carboniferous. *Evol. Ecol. Res.* 4: 779-786

Pubmed: [Author and Title](#)
CrossRef: [Author and Title](#)
Google Scholar: [Author Only](#) [Title Only](#) [Author and Title](#)

Kubec R, Cody RB, Dane AJ, Musah RA, Schraml J, Vattekkatte A, Block E (2010) Applications of direct analysis in real time-mass spectrometry (DART-MS) in Allium chemistry. (Z)-butanethial S-oxide and 1-butenyl thiosulfinates and their S-(E)-1-butenylcysteine S-oxide precursor from Allium sicutum. *J. Agric. Food Chem.* 58: 1121-1128

Pubmed: [Author and Title](#)
CrossRef: [Author and Title](#)
Google Scholar: [Author Only](#) [Title Only](#) [Author and Title](#)

Leonardos G, Kendall D, Barnard N (1969) Odor Threshold Determinations of 53 Odorant Chemicals. *J. Air Pollut. Control Assoc.* 19: 91-95

Pubmed: [Author and Title](#)
CrossRef: [Author and Title](#)
Google Scholar: [Author Only](#) [Title Only](#) [Author and Title](#)

Massa GD, Gilroy S (2003) Touch modulates gravity sensing to regulate the growth of primary roots of Arabidopsis thaliana. *Plant J.* 33: 435-445

Pubmed: [Author and Title](#)
CrossRef: [Author and Title](#)
Google Scholar: [Author Only](#) [Title Only](#) [Author and Title](#)

Netzly DH, Butler LG (1986) Roots of Sorghum exude hydrophobic droplets containing biologically active components. *Crop Sci.* 26: 775-778

Pubmed: [Author and Title](#)
CrossRef: [Author and Title](#)
Google Scholar: [Author Only](#) [Title Only](#) [Author and Title](#)

Okada K, Shimura Y (1990) Reversible root tip rotation in Arabidopsis seedlings induced by obstacle-touching stimulus. *Science* 250: 274-276

Pubmed: [Author and Title](#)
CrossRef: [Author and Title](#)
Google Scholar: [Author Only](#) [Title Only](#) [Author and Title](#)

Penn RE, Block E, Revelle LK (1978) Flash vacuum pyrolysis studies. 5. Methanesulfenic acid. *J. Am. Chem. Soc.* 100: 3622-3623

Pubmed: [Author and Title](#)
CrossRef: [Author and Title](#)
Google Scholar: [Author Only](#) [Title Only](#) [Author and Title](#)

Pickard BG (1973) Action potentials in higher plants. *Bot. Rev.* 39: 172-201

Pubmed: [Author and Title](#)
CrossRef: [Author and Title](#)
Google Scholar: [Author Only](#) [Title Only](#) [Author and Title](#)

Piluk J, Hartel P, Haines B (1998) Production of carbon disulfide (CS₂) from L-djenkolic acid in the roots of Mimosa pudica L. *Plant Soil* 200: 27-32

Pubmed: [Author and Title](#)
CrossRef: [Author and Title](#)
Google Scholar: [Author Only](#) [Title Only](#) [Author and Title](#)

Piluk J, Hartel PG, Haines BL, Giannasi DE (2001) Association of carbon disulfide with plants in the family Fabaceae. *J. Chem. Ecol.* 27: 1525-1534

Pubmed: [Author and Title](#)
CrossRef: [Author and Title](#)
Google Scholar: [Author Only](#) [Title Only](#) [Author and Title](#)

Samudrala D, Brown PA, Mandon J, Cristescu SM, Harren FJM (2015) Optimization and sensitive detection of sulfur compounds emitted from plants using proton transfer reaction mass spectrometry. *Int. J. Mass Spectrom.* 386: 6-14

Pubmed: [Author and Title](#)
CrossRef: [Author and Title](#)
Google Scholar: [Author Only](#) [Title Only](#) [Author and Title](#)

Simons PJ (1981) The role of electricity in plant movements *New Phytol.* 87: 11-37

Pubmed: [Author and Title](#)
CrossRef: [Author and Title](#)
Google Scholar: [Author Only](#) [Title Only](#) [Author and Title](#)

Solouki B, Rosmus P, Bock H (1976) Unstable intermediates. 4. Thioformaldehyde. *J. Am. Chem. Soc.* 98: 6054-6055

Pubmed: [Author and Title](#)
CrossRef: [Author and Title](#)
Google Scholar: [Author Only](#) [Title Only](#) [Author and Title](#)

Song K, Yeom E, Lee SJ (2014) Real-time imaging of pulvinus bending in Mimosa pudica. *Scientific Reports* 4: 6466

Pubmed: [Author and Title](#)
CrossRef: [Author and Title](#)

Google Scholar: [Author Only](#) [Title Only](#) [Author and Title](#)

Suzuki E, Yamazaki M, Shimizu K (2007) Infrared spectra of monomeric thioformaldehyde in Ar, N₂ and Xe matrices. *Vib. Spectrosc.* 43: 269-273

Pubmed: [Author and Title](#)

CrossRef: [Author and Title](#)

Google Scholar: [Author Only](#) [Title Only](#) [Author and Title](#)

Tissier A (2012) Glandular trichomes: what comes after expressed sequence tags? *Plant J.* 70: 51-68

Pubmed: [Author and Title](#)

CrossRef: [Author and Title](#)

Google Scholar: [Author Only](#) [Title Only](#) [Author and Title](#)

Torres M, Safarik I, Clement A, Strausz OP (1982) The generation and vibrational spectrum of matrix isolated thioformaldehyde and dideuterothioformaldehyde. *Can. J. Chem.* 60: 1187-1191

Pubmed: [Author and Title](#)

CrossRef: [Author and Title](#)

Google Scholar: [Author Only](#) [Title Only](#) [Author and Title](#)

van Dam NM, Samudrala D, Harren FJM, Cristescu SM (2012) Real-time analysis of sulfur-containing volatiles in Brassica plants infested with root-feeding *Delia radicum* larvae using proton-transfer reaction mass spectrometry. *AoB Plants* 2012

Pubmed: [Author and Title](#)

CrossRef: [Author and Title](#)

Google Scholar: [Author Only](#) [Title Only](#) [Author and Title](#)

Visnovitz T, Világi I, Varró P, Kristóf Z (2007) Mechanoreceptor cells on the tertiary pulvini of *Mimosa pudica* L. *Plant Signal. Behav.* 2: 462-466

Pubmed: [Author and Title](#)

CrossRef: [Author and Title](#)

Google Scholar: [Author Only](#) [Title Only](#) [Author and Title](#)

Volkov AG, Foster JC, Ashby TA, Walker RK, Johnson JA, Markin VS (2010) *Mimosa pudica*: Electrical and mechanical stimulation of plant movements. *Plant Cell Environ.* 33: 163-173

Pubmed: [Author and Title](#)

CrossRef: [Author and Title](#)

Google Scholar: [Author Only](#) [Title Only](#) [Author and Title](#)

Volkov AG, Foster JC, Baker KD, Markin VS (2010) Mechanical and electrical anisotropy in *Mimosa pudica* pulvini. *Plant Signal. Behav.* 5: 1211-1221

Pubmed: [Author and Title](#)

CrossRef: [Author and Title](#)

Google Scholar: [Author Only](#) [Title Only](#) [Author and Title](#)

Volkov AG, Reedus J, Mitchell CM, Tuckett C, Volkova MI, Markin VS, Chua L (2014) Memory elements in the electrical network of *Mimosa pudica* L. *Plant Signal. Behav.* 9: e982029

Pubmed: [Author and Title](#)

CrossRef: [Author and Title](#)

Google Scholar: [Author Only](#) [Title Only](#) [Author and Title](#)

Watanabe O, Suzuki E, Watari F (1991) Photolysis of thietane and thietane-d₆ in argon matrix: infrared spectra of matrix-isolated thioformaldehyde and thioformaldehyde-d₂. *Bull. Chem. Soc. Jpn.* 64: 1389-1391

Pubmed: [Author and Title](#)

CrossRef: [Author and Title](#)

Google Scholar: [Author Only](#) [Title Only](#) [Author and Title](#)